

Synthesis and Electrochemical Characterization of Cadmium Sulfide-Polyaniline Composite



A dissertation submitted to the Department of Chemistry, Quaid-i-Azam University, Islamabad, as satisfying the partial fulfilment of requirements for the degree of

Master of Philosophy

In

Physical Chemistry

By

FARMAN ULLAH

Reg. No. 02061711040

Department

of Chemistry Quaid-i-

Azam University

Islamabad

Session

2017 _2019

Hadith-e-Qudsi

1377. Ibn Mas`ud (May Allah be pleased with him) reported: The Prophet (PBUH) said, "Envy is permitted only in two cases: Aman whom Allah gives wealth, and he disposes of it rightfully, and aman to whom Allah gives knowledge which he applies and teaches it."

(Al-Bukhari and Muslim)

DECLARATION

This is to certify that this dissertation submitted by *Mr. Farman ullah* is accepted in its present form by the Department of Chemistry, Quaid-i-Azam University, Islamabad, Pakistan, as satisfying the dissertation requirements for the degree of *Master of Philosophy in Physical Chemistry*.

Supervisor:

Dr. Safer Ahmed
Associate Professor
Department of
Chemistry Quaid-i-
Azam University
Islamabad

Head of Section:

Dr. Hazrat Hussain
Department of
Chemistry Quaid-i-
Azam University
Islamabad

External Examiner:

Chairman:

Prof Dr. Shahid Hameed
Department of Chemistry
Quaid-i-Azam University
Islamabad

PLAGIARISM CERTIFICATE

This is to certify that **Farman Ullah (Reg.No.02061711040)** has completed Master of Philosophy in Physical Chemistry, Quaid-i-Azam University Islamabad. The title of his research work is **“Synthesis and electrochemical characterization of cadmium sulfide-polyaniline composite”**. Similarity index of this thesis was checked on Turnitin and was found that its overall similarity index is 13 %.

Supervisor

Dr. Safer Ahmed

Associate Professor

Department of Chemistry

Quaid-i-Azam University Islamabad, Pakistan

AUTHOR'S DECLARATION

The research work presented in this thesis was carried out by me (Farman Ullah) in the Physical Chemistry laboratory (Room No. 6 & 31-A), Department of Chemistry, Quaid-i-Azam University Islamabad. All the findings reported in this thesis are from my own investigations with the approval and membership of my supervisor **Dr. Safer Ahmed**. No part of this work has been presented for any other degree.

FARMAN ULLAH

Dedication

DEDICATED TO,

MY BELOVED PARENTS, BROTHERS

SISTERS, WIFE, FAIZA,

NAVEED, AHMAD

AND FRIENDS.

Acknowledgements

First of all, I pay my gratitude to Almighty Allah, the Lord and Creator of the heavens and earth. He is certainly the supreme patronage of my life. All respects for His last prophet Hazrat Muhammad (S.A.W) who bestowed us the perfect code of life.

*I would first like to thank my advisor, **Dr. Safeer Ahmed** for his guidance and encouragement over the years, and for always reminding me to consider a problem at its most basic, fundamental level. I am particularly grateful for his understanding and support of my involvement in activities outside of the lab, which allowed me to develop the nontechnical skills needed to advance my career. I would also like to extend a special thank you to professor **Dr. Shahid Hameed** (chairman department of chemistry Q.A.U Islamabad, **Dr. Hazrat Hussain** (Head of physical section department of chemistry Q.A.U Islamabad) for their support and precious time. A special thanks to my elder brothers **sabir , Irfan ullah, salman and luqman**.*

*Thank you to all of my amazing lab mates both past and present (**Muhammad Ali, Rabia Ali**) for their support, guidance. I am thankful to all teaching faculty for their best deliverance of knowledge and all staff members of chemistry department for their best cooperation during the tenure of my studies. A huge thank you goes out to all of my friends specially, **Nasreen, Muhammad zulqarnain, Arsalan Hameed, Naimat Ullah, Naveed Ullah and Tufail Dawar**. Because of you all, I have maintained my sanity through this long and strenuous process. I have enjoyed all over our conversations over the years, both technical and personal, and I hope our paths cross again in the future, thank you to, for being the classmates. Finely thanks to QAU for serving the nation by providing the best educational facilities.*

FARMAN ULLAH.

(farmanullah@chem.qau.edu.pk)

Table of Contents

Description Page No.

Contents	i
List of Figures	iv
List of schemes	vi
Abbreviations	vii
Abstract	viii

Chapter

1.....	01
INTRODUCTION.....	1
[1.1] Types of supercapacitors.....	2
[1.1.1] Electrical double layer capacitor.....	2
[1.1.2] Pseudocapacitor.....	4
[1.1.3] Hybrid supercapacitor.....	5
[1.2] Electrode material.....	5
[1.2.1] Carbon based materials for EDLC.....	5
[1.2.2] Carbon nanotubes.....	6
[1.2.3] Activated carbon.....	7
[1.2.4] Graphene.....	7
[1.3] Faradic materials for pseudocapacitive supercapacitor.....	9
[1.3.1] Transition metal oxides.....	9

[1.3.2] Conductive polymers.....	9
[1.4] Cadmiumsulfide.....	11
[1.5] Electrolytes in supercapacitor	11
[1.6] Supercapacitor performance testing.....	11
[1.6.1] Cyclic voltammetry.....	12
[1.6.2] Galvanostatic charge discharge.....	13
[1.7] Electrochemical impedance spectroscopy.....	16
[1.8] Literature review.....	17
[1.9] Aims and objectives.....	18

Chapter

02.....	20
----------------	-----------

Instrumentation and methodology.....	20
---	-----------

[2.1]X-ray Diffraction (XRD).....	21
-----------------------------------	----

[2.2] FTIR analysis	22
---------------------------	----

[2.3] Electrochemical analysis	23
--------------------------------------	----

[2.2]Synthesis procedure.....	24
-------------------------------	----

[2.2.1] Hydrothermal synthesis of CdS.....	24
--	----

[2.2.2] Polyaniline synthesis.....	24
------------------------------------	----

[2.2.3] Ternary composite CdS/GNP/PANI	25
--	----

[2.2.4] Electrode modification.....	26
-------------------------------------	----

Chapter

03.....	27
----------------	-----------

Results and Discussion.....	27
------------------------------------	-----------

[3.1] X-ray diffraction powder analysis	27
---	----

[3.2] FTIR analysis.....	28
[3.3]Cyclic voltammetry of polyaniline.....	29
[3.3.1] Specific capacitance of PANI at various scan rates.....	31
[3.3.2] Energy density calculations of PANI at different scan rates.....	32
[3.4] Cyclic voltammetry of GNP/PANI.....	33
[3.4.1] Specific capacitance and energy density of GNP/PANI.....	35
[3.5] Cyclic voltammetry of CdS/GNP/PANI.....	36
[3.5.1] Specific capacitance and energy densityof CdS/GNP/PANI.....	38
[3.6] Comparison of CV of PANI, GNP/PANI and CdS/GNP/PANI.....	39
[3.7] Comparison of specific capacitance, energy density of PANI, GNP/PANI, CdS/GNP/PANI.....	41
[3.8] Stability of CdS/GNP/PANI.....	42
[3.9] Nature of process-Statistical analysis.....	44
[3.10] Conclusion.....	45
[3.11] REFERNCES.....	46

List of Figures

[Fig 1.1] Different types of supercapacitor.....	02
[Fig 1.2] Mechanism of charge storage by EDLC.....	03
[Fig 1.3] CV of Carbon dots/RGO and galvanostatic charge discharge of same material.....	06
[Fig 1.4] Description of graphite conversion into GO, RGO and graphe.....	08
[Fig 1.5] Different forms of polyaniline.....	10
[Fig 1.6] Applied voltage variation with time & resulting cyclic voltammetry of an ideal capacitor.....	12
[Fig 1.7] A simple circuit which is conneted to a power source with working resistance RL and through an equivalent series resisitance of power source.....	15
[Fig 2.1.1] XRD principal.....	22
[Fig 3.1] XRD of PANI, CdS, CdS/GNP, PANI/GNP, CdS/PANI/GNP and GNPsynthesized by hydrothermal method.....	28
[Fig 3.2] FTIR spectra of PANI, GNP, PANI/GNP and CdS/GNP/PANIsynthesized by hydrothermal method.....	29
[Fig 3.3] Cyclic voltammogram of polyaniline coated on GCE at 50mVs^{-1} in $1\text{M H}_2\text{SO}_4$ as a supporting electrolyte.....	30
[Fig 3.4] CVsof PANI coated on GCE in $1\text{M H}_2\text{SO}_4$ as a supporting electrolyte at different scan rates	31
[Fig 3.5] Specific capacitance of polyaniline at various scan rates.....	32
[Fig 3.6] Energy density of polyaniline at different scanrates.....	33

[Fig 3.7]Cyclic voltammetry of GNP/PANI composite coated on GCE in 1M H ₂ SO ₄ as a supporting electrolyte at 50mVs ⁻¹	34
[Fig 3.8] CVs GNP/PANI composite coated on GCE in 1M H ₂ SO ₄ as a supporting electrolyte at different scan rates	34
[Fig 3.9] Specific capacitance of GNP/PANIat various scan rates.....	35
[Fig 3.10] Energy density of GNP/PANI at various scan rate.....	36
[Fig 3.11]Cyclic voltammetry of CdS/GNP/PANI composite coated on GCE in 1M H ₂ SO ₄ as a supporting electrolyte at 50mVs ⁻¹	37
[Fig 3.12] CVs of CdS/GNP/PANI composite coated on GCE in 1M H ₂ SO ₄ as a supporting electrolyte at various scan rates.....	37
[Fig 3.13] Specific capacitance of CdS/GNP/PANI at various scan rates.....	38
[Fig 3.14] Energy density of CdS/GNP/PANI at various scan rates.....	39
[Fig3.15] Comparison of CV response of PANI, PANI/GNP and CdS/GNP/PANI CV coated on GCE in 1M H ₂ SO ₄ as a supporting electrolyte at 50mVs ⁻¹	40
[Fig3.16] Comparison of CV response of PANI, PANI/GNP and CdS/GNP/PANI CV coated on GCE in 1M H ₂ SO ₄ as a supporting electrolyte at 100mVs ⁻¹	40
[Fig 3.17] Comparison of specific capacitance of PANI, GNP/PANI and CdS/GNP/PANI.....	41
[Fig 3.18] Comparison of energy density of PANI, GNP/PANI and CdS/GNP/PANI.....	42
[Fig 3.19] Stability of CdS/GNP/PANI coated on GCE in 1M H ₂ SO ₄ as a supporting electrolyte at 100mVs ⁻¹ first and 1000 th cycle	43
[Fig 3.20] Specific capacitance of CdS/PANI/GNP vs cycle no	43

[Fig 3.21] Statistical analysis of electrochemical process.....	44
---	----

List of schemes

[2.1] Hydrothermal synthesis of CdS nanoparticles.....	24
[2.2] Polyaniline synthesis at 0°C by chemical oxidative polymerization.....	25
[2.3] Synthesis of CdS/GNP/PANI by hydrothermal and <i>in situ</i> polymerization.	26

Abbreviation and Acronym

C	Capacitance
CdS	Cadmium sulfide
CV	Cyclic voltammetry
CE	Counter electrode
CPs	Conducting polymers
EDLC	Electrical double layer capacitance
EIS	Electrochemical impedance spectroscopy
FTIR	Fourier transform infrared spectroscopy
GCE	Glassy carbon electrode
GNP	Graphene nanoplatelets
GCD	Galvanostatic charge discharge
PANI	Polyaniline
SCE	Saturated calomel electrode
ν	Scan rate

TMOs	Transition metal oxides
XRD	X-ray diffraction spectroscopy
WE	Working electrode

Abstract

Polyaniline is vastly studied material for supercapacitors because of its high theoretical specific capacitance environmental stability. This research work was aimed to fabricate a composite of polyaniline (PANI) and cadmium sulfide (CdS) followed by its modification by graphene nanoplatelets (GNP) to develop a ternary composite electrode. This composite of CdS/GNP/PANI was successfully synthesized through hydrothermal method and confirmed by XRD and FTIR techniques. The electrochemical studies were carried out using cyclic voltammetry (CV) under different set of conditions. The parameters such as specific capacitance and energy density were calculated. Polyaniline alone showed a specific capacitance of 263Fg^{-1} and energy density of 36Whkg^{-1} at 2mVs^{-1} . The binary composite, GNP/PANI, showed specific capacitance of 540Fg^{-1} and the energy density of 75Whkg^{-1} at 2mVs^{-1} . The ternary composite of CdS/GNP/PANI displayed a specific capacitance of 713Fg^{-1} and energy density of 99Whkg^{-1} at 2mVs^{-1} . The stability of this ternary composite was checked for 1000 consecutive cycles and it was found that after 1000 cycles it still retains 82% of its specific capacitance. The improvement in the specific capacitance clearly indicated the role of CdS nanoparticles and GNPs and the outcome is interpreted accordingly.

INTRODUCTION

Electrical energy can be stored electrochemically in two different ways. One is the “faradic process” which is the oxidation reduction of the electrochemically active material. This redox process leads to the electrical work which allows the charges to flow between two electrodes which are at different potentials. This phenomenon is used in batteries. The second way is the “electrostatic” storage which is achieved by the charge separation at the polarized interface. This phenomenon is used in conventional capacitor also called electrolytic capacitor¹. Batteries are of two types primary batteries also called single use (not rechargeable) and secondary batteries (rechargeable)². In secondary batteries where energy is stored reversibly – since energy is stored through faradic reaction (in faradic reaction electrochemical conversion of material occurs). These conversion are usually associated with phase changes. Although the energy storage is due to the thermodynamically reversible process however the charge discharge process in secondary batteries is usually accompanied with volume changes and irreversibility of electrochemical reaction thus leading to the limited life cycle of secondary battery. On the other hand capacitor has almost unlimited cyclability as it is not accompanied with chemical and phase changes during the energy storage process. However, conventional capacitor with the advantage of high cyclability, they are limited with their low energy density($\leq 10^{-2}$ W/Kg). However,if these capacitors are combined with liquid electrolyte and high specific surface area electrode material like graphene, activated carbon and other carbon based materials then they can achieve a high capacitance up to several hundred Farad per gram(F/g) in aqueous electrolyte³. This combination produces another class of storage devices called supercapacitor or ultracapacitor or electrochemical capacitor(EC). So supercapacitor acts as a bridge between conventional capacitors and batteries⁴.

1.1 Types of Supercapacitor

Supercapacitor are further sub-classified into three types. Classification is depicted in Fig.1.1.

- (i) Electrical double layer capacitor (EDLC)
- (ii) Pseudocapacitor
- (iii) Hybrid capacitor.

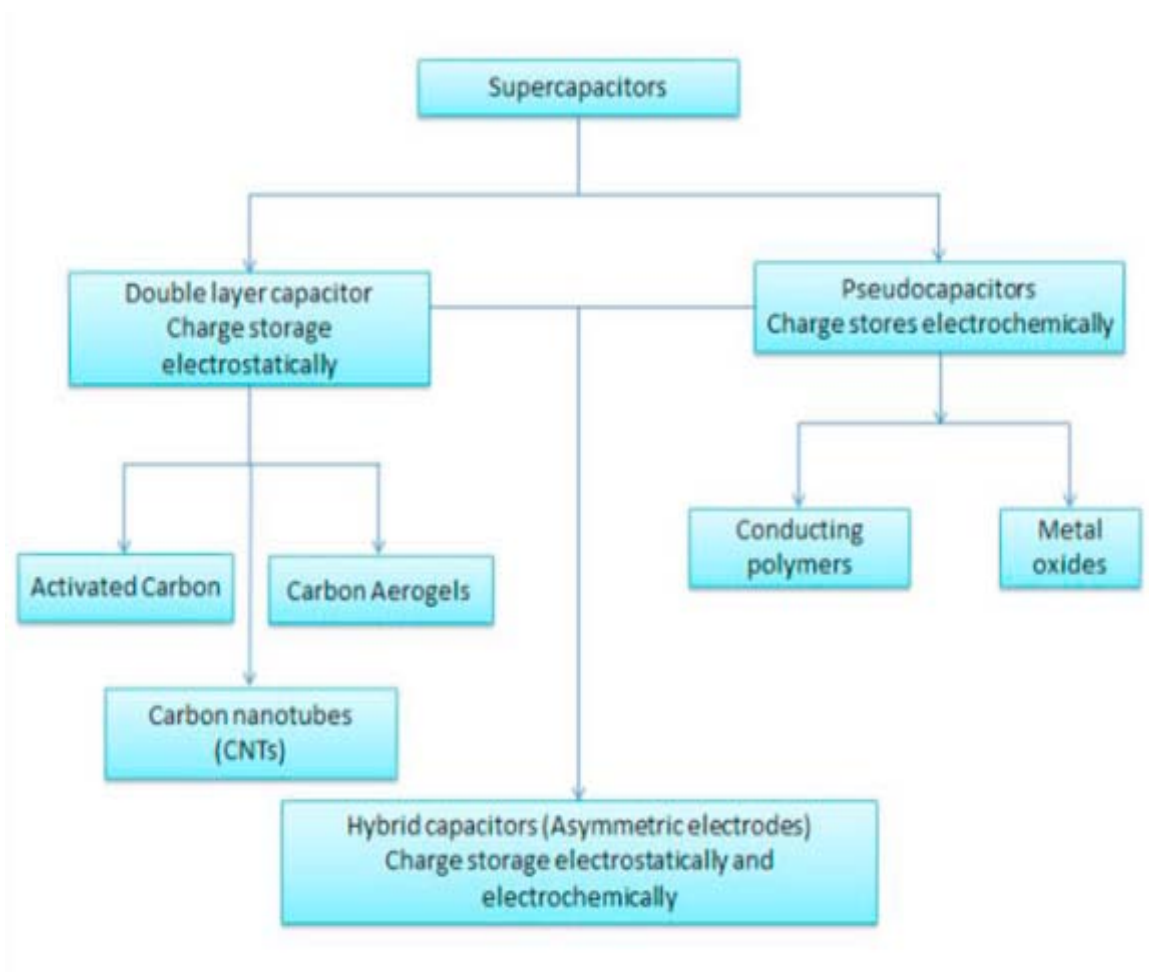


Fig.1.1 Different types of supercapacitor⁵

1.1.1 Electrical double layer capacitor (EDLC)

Carbon materials like carbon nanotubes (CNTs), graphene, reduced graphene oxide (RGO), graphene oxide and activated carbon are used as EDLCs⁶. The EDLCs

have similar structure to that of conventional capacitors(have low energy density),thus storing the charge by a non-faradic process. As there is no electron transfer reactions involved therefore they have no limitation due to electrochemical kinetics(Pseudocapacitor involved electron transfer so they have such limitations). Therefore, EDLC has higher energy and power densities than pseudocapacitor⁷.

Working of electrical double layer capacitor

EDLCs are mostly confused with the electrolytic capacitor(as it also stores charges electrostatically). The conventional capacitor is a dielectric one such as film capacitor and ceramic capacitor these consists of two electrodes which are separated by the dielectric material which store the charges in electrostatic manner. On the other hand EDLC stores the charges by Helmholtz electrical double layer effect in which there is interface of electrode surface /electrolyte positive or negative ions in the electrode against solvated negative or positive ions which are produced by the liquid electrolyte. As electrolytic capacitor also contains electrolyte but its capacitance depends entirely on the oxide films that are present on metal plates by performing an anodic electrolysis thus they become dielectric ones. As EDLC have large surface area than dielectric capacitor and having more smaller separation distance from the molecule separator such as water molecule of an order of 0.3-0.8nm this is smaller than insulating oxide layer of an order of 10-100nm in conventional electrode and thus giving high specific capacitance to EDLC by a factor of 10,000, so there is only adsorption desorption of ions at this large surface area of electrode⁸.

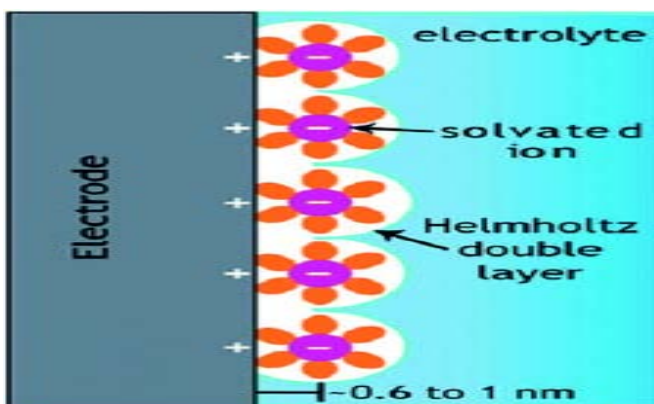


Fig 1.2(Adapted from⁹)Mechanism of charge storage by EDLC

The capacitance C is the amount of charge Q which is accumulated due the change in potential V so for EDLC the capacitance C arises because of physical separation of charges which is described in terms of electrode surface area A , the charge separation distance d and the electrolyte dielectric constant ϵ so

$$C = \frac{\epsilon \times A}{d} \quad (1.1)$$

So as EDLC has large surface area and small separation distance giving it a high capacitance.

1.1.2 Pseudocapacitor

Pseudocapacitors are different from the EDLCs as they involved highly fast and reversible faradic reaction between electrolyte and electrode material. Different metal oxides (MnO_2 , RuO_2 etc) and conducting polymers (polyaniline, polypyrrole etc) show pseudocapacitance behavior¹⁰.

Pseudocapacitors work like rechargeable batteries which involve faradic process and therefore there is confusion between these two types of charge storing devices. Actually charge storage mechanism of pseudocapacitor and battery is quite different. The pseudocapacitor involves a highly fast and reversible faradic (redox) reaction on the surface or close to the surface of electrode material having a distance of $l \ll (2Dt)^{1/2}$ (Here D (cm^2s^{-1}) is diffusion coefficient for the ions and t (s) is time while l is the diffusion thickness. So pseudocapacitor faradic reaction is not affected by diffusion limit and phase transformation of electrode material. Simply, we can say pseudocapacitance is due to the transfer of delocalized electrons while battery capacitance is due to the transfer of localized valence electrons. The pseudocapacitance is produced from three mechanisms (i) under potential deposition (ii) surface controlled electrochemical rapid reactions and (iii) fast ion intercalation. While in batteries the energy is stored in the form of crystal lattice through electrochemical reaction which are affected by the phase transformation, diffusion of reactant molecules/ions and chemical binding changes, thus resulting in more kinetic stagnant, low reversibility and electrochemical process has diffusion controlled kinetics. That is why batteries have low capacitance, power density and short life

cycles than electrochemical supercapacitor¹¹. The theoretical capacitance for the pseudocapacitor can be calculated for metal oxide as

$$C = \frac{n \times F}{M \times V} \text{(1.2)}$$

Here 'n' is the number of electrons involved in faradic process, M is the molar mass of electrode material, V is the operating potential window F is Faraday constant¹².

1.1.3 Hybrid supercapacitor

They are also called battery type or asymmetric supercapacitors. They are formed by combining both EDLCs and pseudocapacitor materials i.e. incorporating metal oxide into graphene or other carbon based materials or incorporating conductive polymers into carbon based materials. So one kind of material stores charge faradaically and other stores charge electrostatically. Hybrid supercapacitor shows high performances in terms of stability, conductivity and specific energy density¹³.

1.2 Electrode materials for supercapacitor

In recent years major progress and practical research has been done on supercapacitor materials but still they have some disadvantages which include high production cost and low energy density. To overcome the disadvantage of low energy density intensive research is going on the development of new electrode materials for supercapacitors.

1.2.1 Carbon based material for EDLC

As stated earlier carbon based materials are suitable for electrical double layer capacitors because of their properties like low cost, high conductivity, environment friendly, good chemical stability, high specific surface area and good performances in wide range of temperature. As shown below in the Fig.1.3 the cyclic voltammogram of carbon based material is rectangular in shape without any redox peaks showing that it stores charge in the form of Helmholtz electrical double layer. The galvanostatic

charge discharge curves of carbon based materials are symmetrical showing high coulombic utility ratio of electrostatic charge storage method¹⁴.

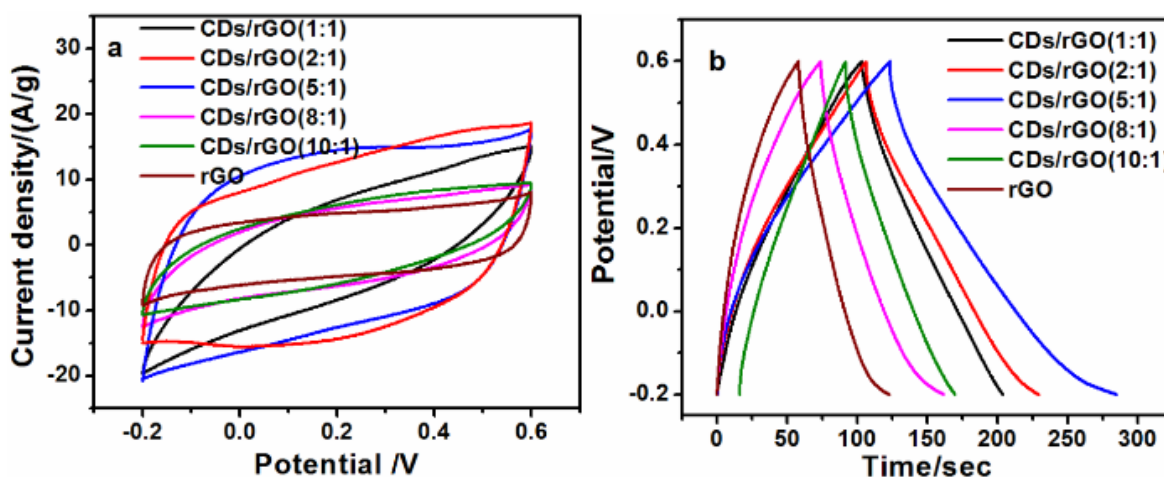


Fig.1.3.(Adapted from¹⁵)(a) cyclic voltammograms of carbon dots/reduced graphene oxide of different composition (b) galvanostatic charge discharge curves of the same materials.

1.2.2 Carbon nanotubes

Carbon nanotubes(CNTs) are superior carbon materials because of their good properties like high conductivity, being thermal and chemical stable and unique porosity. CNT are of two types one is single walled carbon nanotubes(SWCNTs) and second type is known as multi walled carbon nanotubes(MWCNTs). SWCNs are made of single carbon layer having diameter of 0.4-2 nm, depending on which temperature they are synthesized. The single walled carbon nanotubes are of different shapes. They can be arm chair, zigzag, helical or chiral in shape¹⁶. MWCNTs are just like multiple rolled layers (concentric tubes) of graphene. MWCNTs are of two types. One is the parchment-like in which graphene sheet is rolled up around it just like a rolled newspaper the other is called Russian doll model in this model graphene layers are in concentric form¹⁷.

1.2.3 Activated carbon

Activated carbon is popular electrode material for supercapacitor because of its certain properties like low cost, facile processing techniques, easily availability, high surface area (500 to 1500 m²g⁻¹) and high electrochemical stability. These activated carbon materials are produced by physical activation and chemical activation using coke, coal, carbonized organic precursor or chars as primary source. Carbon precursor, time and activation temperature greatly affects the properties of activated carbon such as surface area and distribution of pore size. Activated carbon is also traditionally produced from coals, pitch and petroleum coke but the scarcity of these materials have changed the interest into other inexpensive materials¹⁸.

1.2.4 Graphene

Graphene is a one atom thick, two dimensional, hexagonal sp² hybrid, honey comb allotrope of carbon just like graphite, fullerenes, CNTs. Graphene possess tremendous properties like thermal stability, high mechanical strength (~1TPa) and high conductance. In addition to these graphene exhibits high theoretical specific surface area (~2630 m²/g) making it a good candidate for electrical double layer capacitors¹⁹.

Graphite, Graphene Oxide (GO), reduced Graphene Oxide (RGO) and Graphene nanoplatelets (GNP)

- **Graphite** is a two dimensional carbon layered material but it is not one atom thick. This material can also be used for supercapacitor material but with low capacitance.
- **Graphene oxide (GO)** is one of them which can be produced from the oxidation of graphite using Hummer's method. Graphene oxide has some oxygen functionalities like hydroxyl (OH), carbonyl (C=O) and epoxy (C-O) and therefore its properties are not like pristine graphene. This GO can be easily converted into reduced forms in order to improve its certain properties like conductivity, specific capacitance etc.
- **Reduced graphene oxide (RGO)** is the reduced form of GO. This reduction can be done chemically, electrochemically and thermally.

- **Graphene Nanoplatelets(GNPs)** consist of small stacks of graphene i.e. few layer graphene²⁰.The Fig.1.4 below shows schematic representation of all these conversion processes.

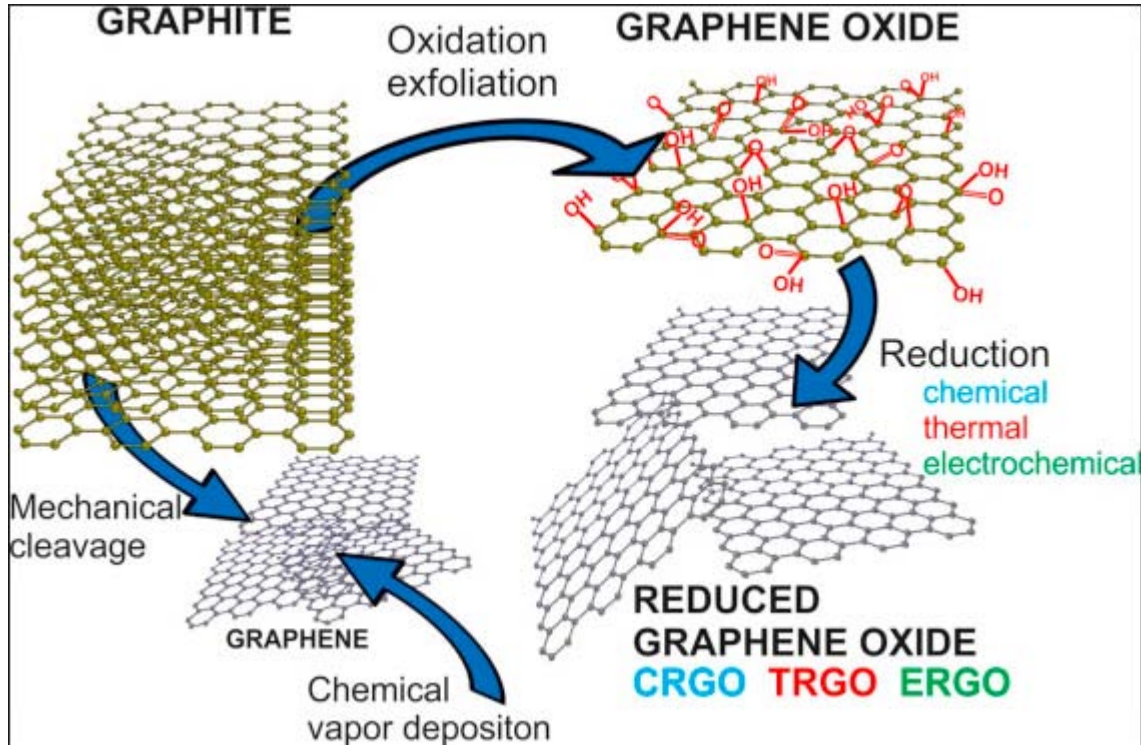


Fig.1.4.Description of graphite conversion into GO, RGO and graphene²¹

For energy storage and other applications some research work is still continued on the synthesis of graphene sheets which can be of different types like (i) CVD and epitaxial growth (ii) chemical exfoliation in organic solvents (iii) mechanical cleavage of graphite and many more. The reported graphene based EDLC have achieved specific capacitance of 154 F/g by hydrazine chemical reduction and with microwave exfoliation 166 F/g²². Recently, graphene composite with pseudocapacitive materials like transition metal oxides (TMOs) and conducting polymers composite are studied. Different graphene conductive polymer composite like graphene polyaniline, graphene polypyrrole and other have been studied. Graphene and metal oxides composites like graphene MnO₂, graphene RuO₂ and many more have been studied²³.

1.3 Faradic materials for pseudocapacitive supercapacitors

As the pseudocapacitor belongs to supercapacitor family however on performance perspectives they are redox materials as like batteries. So same class of materials are used for batteries and supercapacitors, however their working mechanism is different as discussed earlier. There are diversity of faradic electrode materials like TMOs, transition metal chalcogenides (TMCs) and conducting polymers²⁴.

1.3.1 Transition metal oxides (TMO)

Transition metal oxides are also considered as good electrode materials for supercapacitor application because of some advantages like their high specific capacitance which is coupled with low resistance giving them high specific power and high energy density. The conditions for TMO as supercapacitor material are (i) TMO should be conductive, (ii) the proton can freely intercalate in the oxide lattice when it is reduced, allowing easy interconversion of $O^{2-} \leftrightarrow OH^{-1}$, (iii) the TMO can exist in two or more oxidation states without involving any phase changes. Among the most studied transition metal oxides RuO_2 is the best promising material for supercapacitor application because of long life cycle, good electrochemical reversibility, high conductivity and high specific capacitance. However, low natural abundance and high cost make it difficult for commercial application. So lot of alternative TMO materials like NiO , MnO_2 , Fe_3O_4 , V_2O_5 , TiO_2 have been reported¹⁴.

²⁵.

1.3.2 Conductive polymers (CPs)

Conductive polymers are environment friendly, low cost, high conductivity in doped state, wide potential window, high chemical reversibility, high porosity, high storage capacity, extensive source thus making them promising electrode materials as supercapacitor. CPs show capacitance behavior because of their redox reactions. When these conductive polymers are oxidized the ions are shifted to polymer backbone and when it is reduced the ions are shifted from polymer backbone back to the solution. So as these redox reactions do not involve any structural changes like phase changes thus these process are highly reversible in nature¹⁴.

The most common conductive polymers are polypyrrole (PPy), polyaniline (PANI), Poly(3,4-ethylenedioxythiophene) (PEDOT) and polythiophene (PTh). The electronic conductivity in these polymers is introduced by either oxidizing or reducing them and this process is known as ‘doping’. When the polymer is positively charged by oxidizing them are termed as ‘p-doped’. PANI and PPy are p-doped polymers. When the polymer is negatively charged by reducing them and are termed as n-doped polymers. PTh is n-doped polymer. The doping process can be achieved during polymer synthesis by electrochemical or chemical methods, or post polymerization like ion implantation. However, electrochemical and chemical methods are preferable because of low cost and room temperature processing^{14, 26}.

Polyaniline

Polyaniline has been extensively studied as pseudocapacitor material and has theoretical specific capacitance of 2000F/g. The advantages associated with polyaniline are environmental stability, high electrical conductivity, low cost and easy synthesis.

It also offers some disadvantages like volumetric shrinkage, low conductivity in de-doped state. Polyaniline exists in the following three different forms. Leucoemeraldine is the form of polyaniline in reduced state. Emeraldine is the partially oxidized form of polyaniline while pernigraniline is the fully oxidized state of polyaniline²⁷.

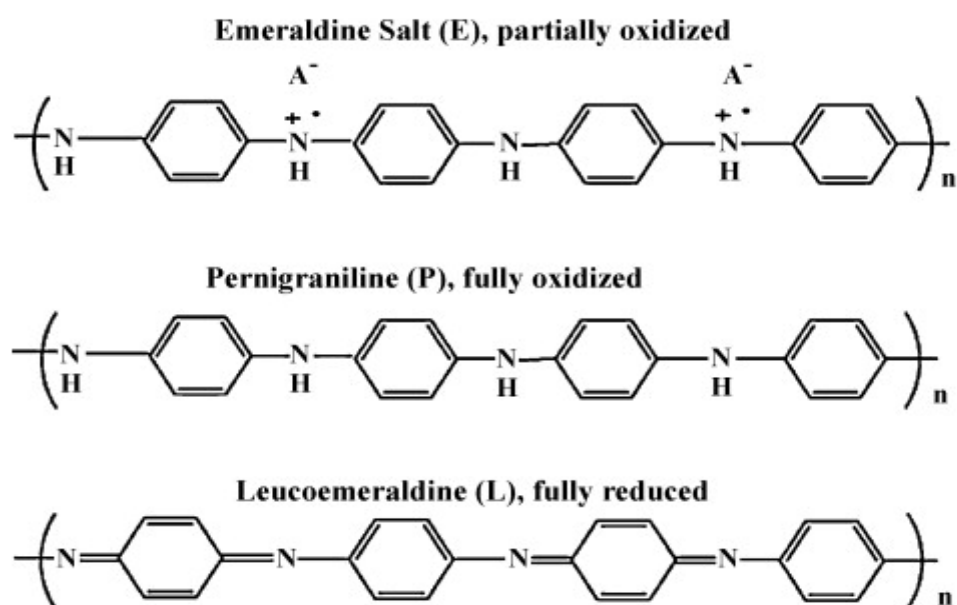


Fig 1.5. Different forms of polyaniline

1.4 Cadmium sulfide

Among the most studied metal sulfides CdS is a good candidate for energy storage applications because of its some unique properties. CdS is an n-type semiconductor with band gap of 2.4eV. It is most studied in cadmium-nickel batteries which show high cycle life, good environmental stability, high discharge rates, relatively less toxicity and high energy density. CdS shows a high theoretical specific capacitance of 1675F/g showing its charge storage ability

1.5 Electrolytes in supercapacitor

Besides the electrodes supercapacitor also involves an electrolyte. This electrolyte should have high electrochemical stability, low resistivity, wide potential range, low volatility, high ionic concentration, cost effective, low toxicity and available in high purity¹⁴. The electrolytes are of three types (i) aqueous electrolytes (ii) organic electrolytes (iii) Ionic liquids

Aqueous electrolytes like H₂SO₄, Na₂SO₄, KOH give low resistance and high ionic concentration than organic electrolytes. Aqueous electrolytes can easily be prepared in pure form. However, there is one disadvantage with aqueous electrolytes that their potential window is very small which is about 1.2V much smaller than organic electrolytes.

On the other hand organic electrolytes have wide potential window as high as 3.5V making them promising candidates for supercapacitor. Commonly used organic electrolytes are propylene carbonate and acetonitrile. The main issue with organic electrolyte is the water content that needs to be below 3-5 ppm¹⁴.

The melted or liquefied salt is called ionic liquid. The properties of ionic liquids are; wide potential range upto 6V, typically about 4.5V, high chemical and thermal stability. Commonly studied ionic liquids are imidazolium and pyrrolidinium based salts²⁹.

1.6 Supercapacitor performance testing

The testing of supercapacitor material can be checked in two ways, two electrode or three electrode cell configuration. The three electrode assembly enables the measurements of electrochemical reactions which are occurring at one electrode and

this electrode under study is called working electrode (WE). Another electrode called counter electrode (CE) completes the electrochemical circuit while reference electrode (RE) gives a constant reference point for the potential measurements. A potentiostat measures the current flow between WE and CE, and the potential difference between WE and RE³⁰.

1.6.1 Cyclic Voltammetry (CV)

cyclic voltammetry is an electrochemical technique of three electrode cell in which WE is cycled between potential V_1 and V_2 at a fixed scan rate and the resulting current of electrode is measured. Fig.1.6 (a) shows the potential changes on WE as a function of time (t) in Fig.1.6 (b) the resulting voltammogram is shown.

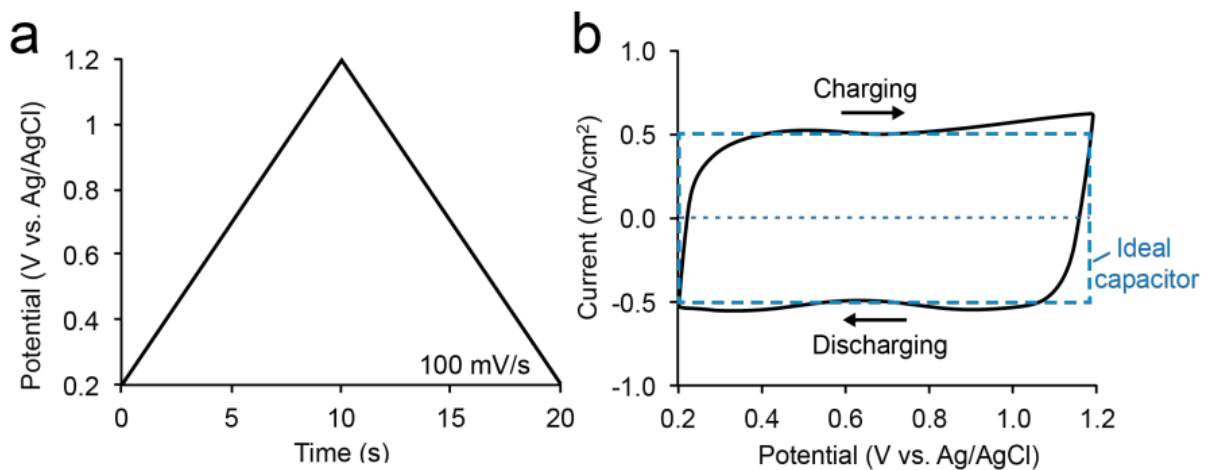


Fig.1.6. (Adapted from³¹) (a) Applied voltage variation with time (b) voltammogram for an ideal capacitor.

The capacitance is given as

$$C = \frac{Q}{V} \quad (1.3)$$

Here C is capacitance, Q is charge while V is voltage.

The Eq. 1.3 can be converted into other forms in order to fit with the experimental data. The common experiment is the current response to voltage variations (as in cyclic voltammetry) so Eq. 1.3 can be rearranged as

$$Q = C \times V \quad (1.4)$$

This Eq.1.4 can be differentiated with respect to time while keeping C as constant

$$\frac{dQ}{dt} = \frac{CdV}{dt} + \frac{VdC}{dt} = \frac{CdV}{dt} \quad (1.5)$$

So if the voltage changes linearly with time i.e $V=V_0 +V_t$ and t is the time V_0 is the initial voltage which may be zero and v is the voltage scan rate so $\frac{dV}{dt} = v$ and

$$\frac{dQ}{dt} = i(\text{current})$$

So Eq.1.5 can be simplified as

$$I = C. v \quad (1.6)$$

Eq. 1.5 gives a rectangular plot between current and voltage which is called cyclic voltammogram as show above in Fig.1.4(b).

Eq. 1.5 can be rearranged to

$$C = \frac{i}{V} \quad (1.7)$$

To find capacitance first find voltammetric charge which can be obtained by integrating the current over the potential scan range and then by dividing $V_2 -V_1$ (V_1 and V_2 are the switching potentials). Dividing also with scan rate and active mass of material gives the capacitance.

$$C = \frac{\int_{V_1}^{V_2} i dv}{2m v (V_2 - V_1)} \quad (1.8)$$

Here 'm' is the mass of active material small 'v' is the scan rate.

1.6.2 Galvanostatic charge discharge (GCD)

This is a two electrode assembly where the one electrode material is charged by applying a constant current to a desired voltage and then discharged until the cell

voltage is zero at constant current as shown in the above Fig.1.3(b).So the capacitance from discharge curve can be obtained as

$$C = \frac{i}{\left[\left(\frac{dv}{dt}\right) m\right]} \quad (1.9)$$

Here $\frac{dv}{dt}$ is the slope of discharge curve. As this curve is considered linear so $\frac{dv}{dt}$ is close to its mean value $(\Delta V/\Delta t)$, Δt is the time in which potential decreases. So Eq.1.9 can be written as

$$C = i \frac{\Delta t}{\Delta V m} \quad (1.10)$$

Here i is the current at which charging discharging takes place while V is the potential window and m is the mass of electrode material.

Energy density and power density

A capacitor is capable to store energy so when a potential V is applied for a short period of time so a small amount of work dW is done by storing a small amount of charge dQ . this work is the product of charge Q and voltage V i.e.

$$dw = V dQ \quad (1.11)$$

By using Eq.1.4, Eq. 1.11 can be written as

$$dw = \frac{Q}{C} dQ \quad (1.12)$$

Now integrating the above Eq.1.12

$$W = \int_0^Q \frac{Q}{C} Dq = \frac{1}{2C} Q^2 \quad (1.13)$$

Using Eq.1.4 again Eq 1.13 changes to

$$W = \frac{CV^2}{2} \quad (1.14)$$

This work can be assumed as the energy stored so energy density is

$$E = \frac{CV^2}{2m} \text{(1.15)}$$

Supercapacitor power (consumption of energy per unit time) can be calculate as

$$P = \frac{E}{t} = \frac{CV^2}{2mt} \text{(1.16)}$$

For maximum power density calculations we can't use above equation so we use

$$P = iV = i^2R \text{(1.17)}$$

The electric power source which is the supercapacitor has some internal resistance called equivalent series resistance (ESR). Now consider a supercapacitor is connected to some load resistance R_L through the circuit as shown below in Fig.1.7.

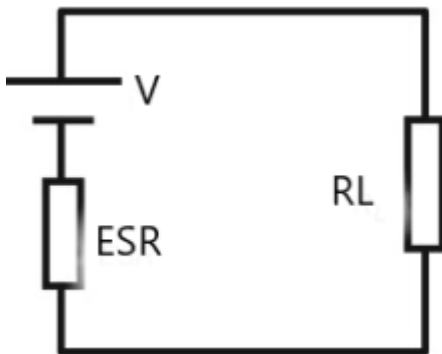


Fig.1.7.(Adapted from ³¹)A simple circuit which is conneted to a power source with working resistance R_L and through an equivalent series resistance of power source.

So the current of power source will be

$$i = \frac{V}{R} \text{(1.18)}$$

Where $R = R_L + ESR$ so Eq. 1.18 becomes

$$i = \frac{V}{R_L + ESR} \text{(1.19)}$$

Putting Eq.1.19 in Eq.1.17 we get

$$P = \left(\frac{V}{R_L + ESR} \right)^2 R_L \quad (1.20)$$

So power will be maximum if R_L is equal to ESR and Eq 1.20 becomes

$$P_{max} = \frac{V^2 ESR}{(ESR + ESR)^2} = \frac{V^2}{4ESR} \quad (1.21)$$

Eq.1.21 shows an interesting thing that the maximum power is dependent on the voltage and ESR but it is independent of capacitance C and it is the C that determines the amount of charge stored. However, the discharging time (T) is dependent on the capacitance C which is as

From Eq. 1.16 rearranging we get

$$T = \frac{CV^2}{2P_{max}} \quad (1.22)$$

Putting Eq.1.21 in above we get

$$T = \frac{CV^2}{2 \left(\frac{V^2}{4ESR} \right)} = 2C ESR \quad (1.23)$$

The Eq.1.23 describe an important parameter for designing the supercapacitor. However, in the present literature reports the supercapacitor performance in terms of Eq.1.21^{27a, 31}.

1.7 Electrochemical impedance spectroscopy (EIS)

Electrochemical impedance spectroscopy which is also called dielectric spectroscopic testing is an important tool for the investigation of the capacitive behavior or to investigate the interfacial or pseudo-capacitance of the supercapacitor material. It provides information such as the capacitance over a range of frequency, equivalent series resistance and any faradic resistance which is potential dependent³². The EIS gives data graphically either in bode plot which is in terms of phase angle and

frequency or a Nyquist diagram in which imaginary plot of impedance is plotted verses the real part of impedance¹⁴.

1.8 Literature Review

For supercapacitor carbon based materials, CPs and transition metal oxides/hydroxides are widely studied. It is found that carbon based materials shows less specific capacitance due to the surface dominant double layer storage process. Transition metal oxides or hydroxides and conducting polymer shows higher capacitance because of redox reactions but their conductivities are too low so cannot support fast electron transport. So it is essential to develop new materials which have properties of high conductance, high specific capacitance and porous structure.

Xu et al. reported (2016) that CdS when coated on nickel foam showed a specific capacitance of 909F/g at 2 mA cm⁻²³³. Nair et al. reported (2018) CdS@HgS core shell nanowires grown on stainless steel current collector. The synthesized materials shows a specific capacitance of 224.97 F/g at a scan rate of 5mVs⁻¹ which retains 87% of its specific capacitance after 1250 cycles³⁴. Adhikar et al. reported (2018) a nanohybrid of CdS-CoFe₂O₄@RGO. This composite shows a specific capacitance of 1487 F/g at 5A/g current density and retains 78% of its capacitance after 5000 cycles . Patil et al. reported (2018) the Co₃O₄@CdS core shell on nickel foam which exhibit the specific capacitance of 1539 F/g at 10mVs⁻¹ and retains 98% specific capacitance after 2000 cycles . Chen et al. reported (2018) CdS anchored in three dimensional graphite cage showing specific capacitance of 511 F/g at 5A/g and retains its 90.1% capacitance after 5000 cycles at 10A/g ³⁶. Patil et al. reported (2018) silver nanowires@ Cadmium sulfide core shell having capacitance of 2662 mFcm⁻² at 10mVs⁻¹³⁷.

Polyaniline is one of the pioneering conducting polymer that can be synthesized by both chemically and electrochemically. Polyaniline has a high theoretical specific capacitance of 2000F/g. Arbizzani and her co-workers(1996) were the first who describe the supercapacitor performance of polyaniline as a result of redox reaction separating it from charge separation at double layer³⁸. Kwang et al. reported (2002) polyaniline doped with HCL and LiPF₆ and shows a specific capacitance of 40 F/g after 400 cycles ³⁹. Chen et al. reported (2003) polyaniline coated on carbon electrode showing specific capacitance of 180 F/g ⁴⁰. Gupta et al. reported

(2006) electrochemically synthesized polyaniline nanostructure of 755 F/g at 10 mVs⁻¹¹⁴¹. Dhawale et al. (2011) synthesized nanostructured polyaniline with specific capacitance of 503 F/g at 10 mVs⁻¹¹⁴². Khdary et al. reported (2014) mesoporous polyaniline films with specific capacitance of 532 F/g at 1.5 A g⁻¹¹⁴³.

Polyaniline/Graphene composite have also been studied for supercapacitor performance. Feng et al. showed (2011) that the composite of polyaniline and graphene using aniline and graphite oxide as starting material. This composite showed a specific capacitance of 640 F/g at 0.1 A/g⁴⁴. Ma et al. reported (2012) the composite of PANI vertically aligned on the sulfonated graphene through an interfacial polymerization method. This composite shows a specific capacitance of 497 F/g at 0.2 A/g⁴⁵.

Ternary composite for supercapacitor results in better performance because these three components not only enhance each other but also have potential synergy. Yu et al. reported (2014) the ternary composite of MnO₂, polyaniline and graphene showing the specific capacitance of 755 F/g at 0.5 A/g. After 1000 cycles it still retains 87% of its specific capacitance⁴⁶. Kumar et al. reported (2015) ternary composite of MoO₃/GNP/PANI showing larger specific capacitance of 593 F/g at 1 A/g with 92% retention of its specific capacitance after 1000 cycles⁴⁷. Li et al. reported (2016) the ternary composite of MoS₂, polyaniline and reduced graphene oxide with high specific capacitance of 1224 F/g at 1 A/g⁴⁸. Purty et al. (2018) synthesized ternary composite of CdS, polypyrrole and reduced graphene oxide which shows high specific capacitance of 844 F/g at 1 A/g. This composite retains its 92.8% of specific capacitance after 2000 consecutive cycles⁴⁹.

1.9 Aims and Objectives

This project aims to prepare CdS/PANI/GNP composite to investigate its

charge storage application. The sequential targets were;

- (i) The synthesis of CdS nanoparticles and PANI followed by the synthesis of binary composite of CdS/PANI with modification of commercial graphene nanoplatelets.
- (ii) Structural characterizations of the synthesized composite by XRD and FTIR.

- (iii) Electrochemical study of the material for its faradic and capacitive behavior by employing cyclic voltammetry.
- (iv) Interpretation of the results for the use of synthesized material as electrode in supercapacitor devices.

Chapter 2 Experimental

Instrumentation and methodology

All the chemicals were used as received without any further purification or distillation process. All solutions as well as solutions prepared for cyclic voltammetry were prepared in deionized water (DI). All the following chemicals mentioned in Table.2.1 were used.

Table2.1List of chemicals used in research work

Seri al No	Chemical names	Chemical formulas	Formula Weight g/mol	%age Purity	Source
1	Aniline	$C_6H_5-NH_2$	93.13	98	BDH Chemicals
2	Sulfuric acid	H_2SO_4	98.079	95-97	BDH chemicals
3	Ammonium per sulfate	$(NH_4)_2 S_2O_8$	228.18	98	Sigma Aldrich
4	Cadmium nitrate	$Cd(NO_3)_2.4H_2O$	308.48	99.9	BDH chemicals
5	Sodium sulfide	$Na_2S.9H_2O$	240.22	97	BDH chemicals
6	N,N-dimethylformamide	C_3H_7NO	73.09	99.8	Sigma Aldrich

7	CTAB	C ₁₉ H ₄₂ BrN	364.45	99	Sigma
8	Graphene nanoplatelets		-	99.9	ACS material store
9	Acetone	C ₃ H ₆ O	58.08	99.98	Sigma Aldrich
10	Ethanol	C ₂ H ₅ OH	46.07	99	Sigma Aldrich
11	De-ionized water	H ₂ O	18		
12	Nafion	C ₇ HF ₁₃ O ₅ S. C ₂ F ₄	544	5	Sigma Aldrich

2.1 X-ray diffraction (XRD)

XRD is rapid nondestructive method employed for determination of crystal size(crystallinity) of compound equally applicable to liquid, powder and crystals. X-ray diffractometer model analytical 30440/60 X pert PRO of Spectris company Australia is used to analyse synthesized material.

X-ray diffraction works on the principle of constructive interference of X-rays and crystalline material. In this interference diffracted rays are produced which follow Bragg's Law($n \lambda = 2d \sin \theta$)⁵⁰. This law gives relationship between wavelength of electromagnetic radiation to the diffraction angle and the lattice spacing in a crystalline material. Then detection of these diffracted rays then processed and counted. Scanning at different 2θ angles is done due to random orientation of particles diffraction in different direction is done. These diffraction peaks are studied for identification of the crystalline material because each crystalline material has its own set of particular d-spacings. This identification process is done by comparing d-spacings with some standard reference patterns.

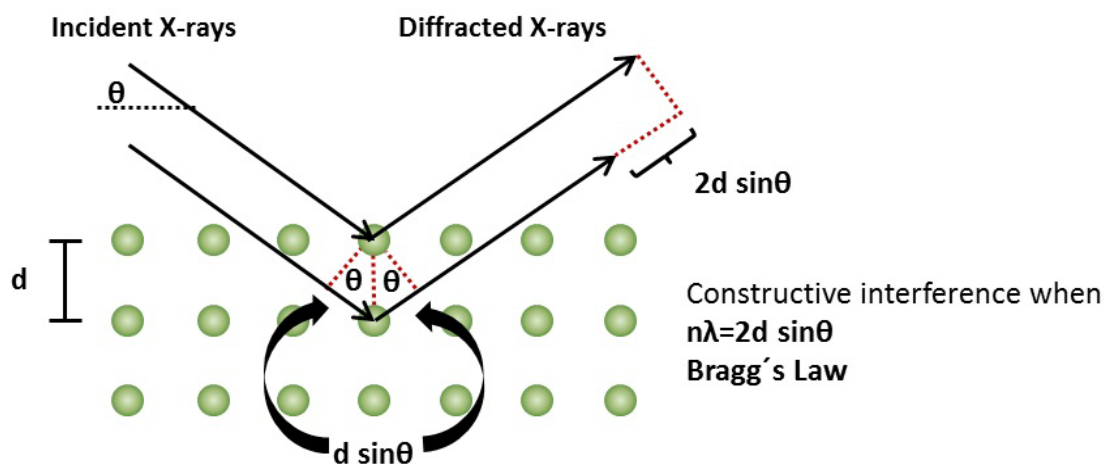


Fig.2.1 XRD principle [56].

Crystal size measurement

Size measurement of particles is done using Debye Scherrer equation as

$$D = \frac{K\lambda}{\beta \cos \theta} \quad (2.1)$$

D = size of particle, K = shape factor, λ = wavelength of X-ray, β = full wave half width and θ is diffracted angle.⁵¹

2.2 FTIR Analysis

FTIR analysis is done to identify various compounds, using infrared light to scan the sample and identify chemical bonds of given sample. Using Alpha-FTIR spectrometer of Bruker Company, in frequency range $400\text{-}6000\text{cm}^{-1}$ identification of synthesized sample is done.

Transmission technique is employed for FTIR analysis, light is focused on sample that is inserted into optical path length, the light that is directed over sample at different angles cause the phenomenon of internal reflection and then bounces back from top and bottom of crystal. Energy interactions occur between the interface of sample and crystal and bounce position is located. More energy transfer occurs where the large bounce takes place⁵².

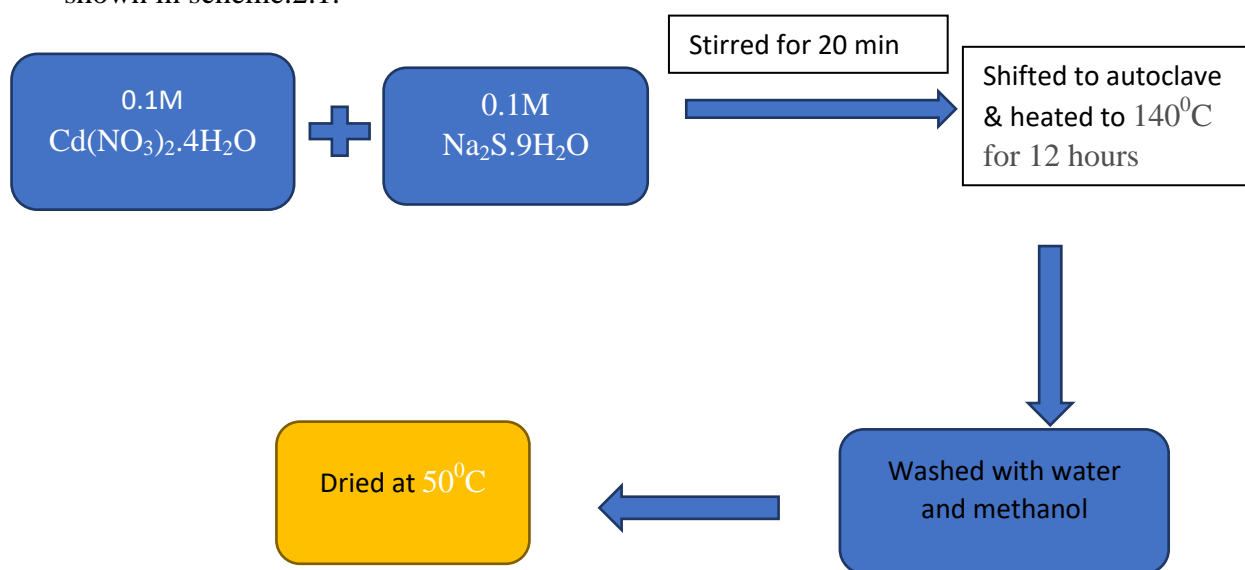
2.3 Electrochemical analysis

Gamry 1000E interface instrument was used for the electrochemical performance of the electrode material. Three electrode system is employed using glassy carbon with 0.0707 cm² area coated with 0.1mg of different composite materials as working electrodes, calomel electrode (Hg/Hg₂SO₄) as reference one and Pt wire as counter electrode. All the cyclic voltammetry performance done in this work were carried out within the potential window from -0.1 to 0.9 V in 1M H₂SO₄ as electrolyte. All the scan were carried out starting from less positive potential to more positive potential.

2.4 Synthesis procedure

2.4.1 Hydrothermal synthesis of CdS

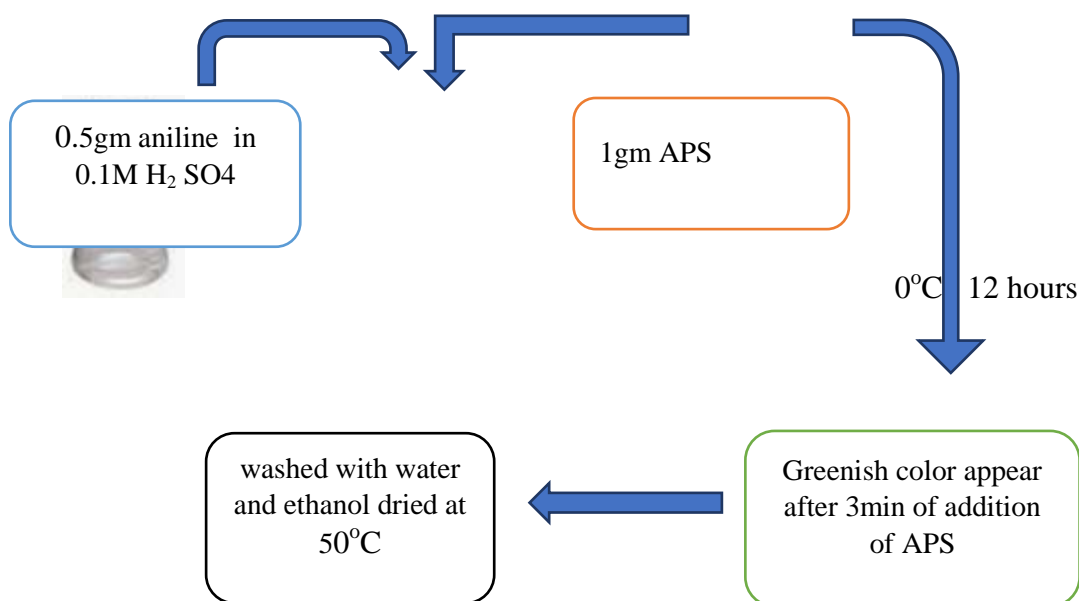
CdS nanoparticles were synthesized through a hydrothermal procedure. In this procedure 10ml of 0.1M $\text{Cd}(\text{NO}_3)_2 \cdot 4\text{H}_2\text{O}$ and 10 ml of 0.1M of $\text{Na}_2\text{S} \cdot 9\text{H}_2\text{O}$ were prepared and then mixed and kept it for stirring for 20 minutes. Then this mixture was shifted to autoclaves where they were heated at 140°C for 12 hours. After 12 hours it was washed with deionized water and methanol and then dried at 50°C for 5 hours, shown in scheme.2.1.



Scheme.2.1 Hydrothermal synthesis of CdS nanoparticles

2.4.2 Polyaniline synthesis

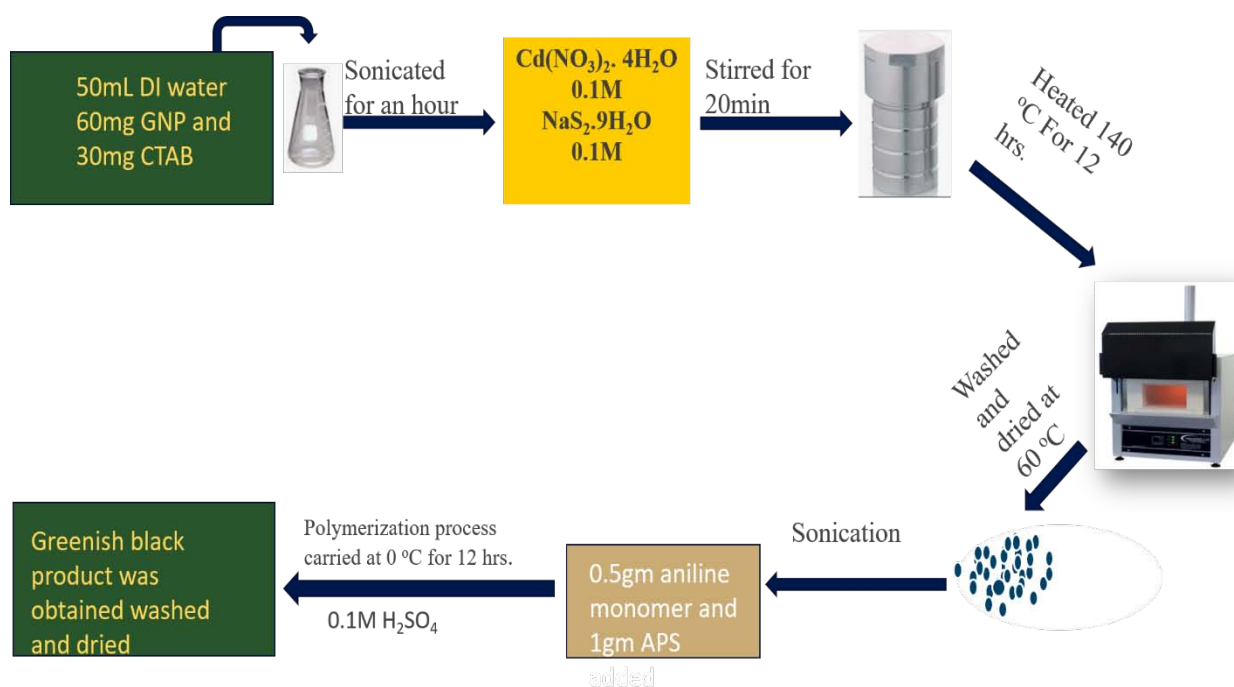
Polyaniline polymer was synthesized using an oxidative chemical polymerization process. First of all 0.5gm of aniline was taken and dispersed in 100 ml of 0.1M H_2SO_4 . Then 1gm ammonium persulfate (APS) initiator was added drop wise. This whole process was carried at 0°C for 12 hours. Sulfuric acid used in this scheme for doping of polyaniline (doped polyaniline has better conductivity). After 12 hours of reaction completion the product was washed with DI water and ethanol and dried at 50°C for 12 hours, shown in scheme 2.2.



Scheme 2.2 Polyaniline synthesis at 0°C by chemical oxidative polymerization

2.4.3 Ternary composite CdS/GNP/PANI synthesis

For ternary composite synthesis first of all 60mg graphene nanoplatelets (GNP) and 30mg cetyltrimethylammonium bromide (CTAB) was added to 20ml DI water and sonicated for an hour. Sonication and CTAB was used for dispersion of GNP. Cadmium nitrate 0.1M and sodium sulfide 0.1M was added to this mixture and stirred for 20 minutes. It was shifted to autoclave and heated to 140°C for 12 hours. After heating it was washed with DI water and ethanol and dried at 50°C for 6 hours. Then this product was again sonicated in 100ml DI water. To this sulfuric acid was added to this to make it 0.1M acidic solution. Aniline monomer 0.5 gm was added followed by drop wise addition of APS initiator and this polymerization step was carried at 0°C for 12 hours. Again it was washed with DI water and ethanol and dried at 50°C for 6 hours, shown in scheme 2.3.



Scheme 2.3 Synthesis of CdS/GNP/PANI by hydrothermal and *in situ* polymerization

For comparison study other composite like CdS/GNP, GNP/PANI were also synthesized by the same method.

2.4.4 Electrode modification

The cyclic voltammetry was performed on glassy carbon electrode (GCE) acting as working electrode. This GCE was modified with the synthesized material. In this modification process 1mg of active material, $100\mu\text{L}$ DMF and $5\mu\text{L}$ Nafion was sonicated for 20 minutes and then $10\mu\text{L}$ was drop casted on GCE and then dried. This was used as modified.

CHAPTER 3

RESULTS AND DISCUSSION

This chapter describes the results, the obtained data from therein and their interpretation in the context of set objectives and hypothesis of the work.

3.1 X- ray powder diffraction analysis

Fig.3.1 shows XRD pattern of all the synthesized composites. Polyaniline shows a broad peak at 25.4° of 2θ with (112) plane. Graphene nanoplatelets (GNP) show a sharp characteristic peak at 26.1° of 2θ with (002) plane. Cadmium sulfide shows three diffraction peaks at $26.3, 43.5$ and 51.6 which were assigned to the (1 1 1), (2 2 0), (3 1 1) planes and these peaks are consistent with standard data files of JCPDS # 00-001-0647. This XRD of CdS confirms that synthesized CdS is cubic in nature⁵³. The CdS/GNP composite shows the three characteristic peaks of CdS and a small hump at 25.05 of 2θ for GNP. PANI/GNP composite shows their characteristic peaks. The XRD of ternary composite of CdS/PANI/GNP shows all the characteristic peaks for CdS, GNP and polyaniline.

From the given XRD pattern of composite it can be deduced that the crystallinity of CdS has increased as indicated by the peak intensities of pure CdS and peak intensities of CdS in ternary composite (peak intensities in ternary composite has increased). The grain size of synthesized CdS was calculated applying the Scherrer equation (Eq.2.1) ⁵⁴ and it was found to be 15nm.

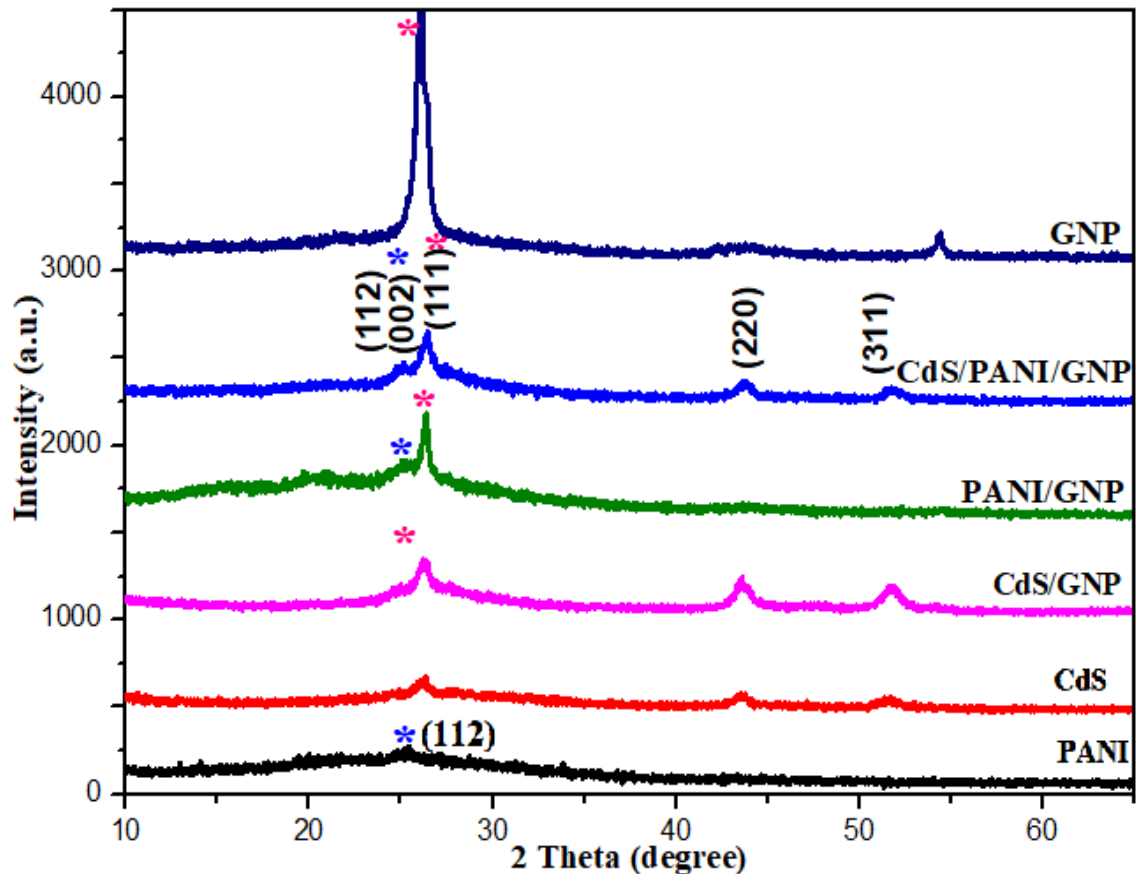


Fig.3.1.XRD of PANI, CdS, CdS/GNP, PANI/GNP, CdS/PANI/GNP and GNPs synthesized by hydrothermal method.

3.2 FT-IR analysis

The formation of polyaniline and ternary composite (CdS/GNP/PANI) was also confirmed by the FTIR analysis. The polyaniline FTIR spectrum as shown in Fig.3.2 shows the characteristic peaks at 1480 and 1557cm^{-1} which are due to stretching vibrations of the quinoid and benzenoid rings respectively. The peaks at 787 and 1040cm^{-1} are attributed to the sulfate group which are attached to the aromatic rings confirming successful doping of polyaniline⁵⁵. GNP FTIR shows its characteristic peaks at 1738 and 1366cm^{-1} which are due to stretching vibrations of C=O, C-OH stretching in GNP. The small peaks observed at 1587 - 1645cm^{-1} due to the C=C stretching vibrations of graphene flakes. In the FTIR spectrum of ternary composite of CdS/GNP/PANI all the characteristic peaks for GNP and polyaniline are present. The peaks at 412 and 626cm^{-1} are due Cd-S bond stretching⁵⁶.

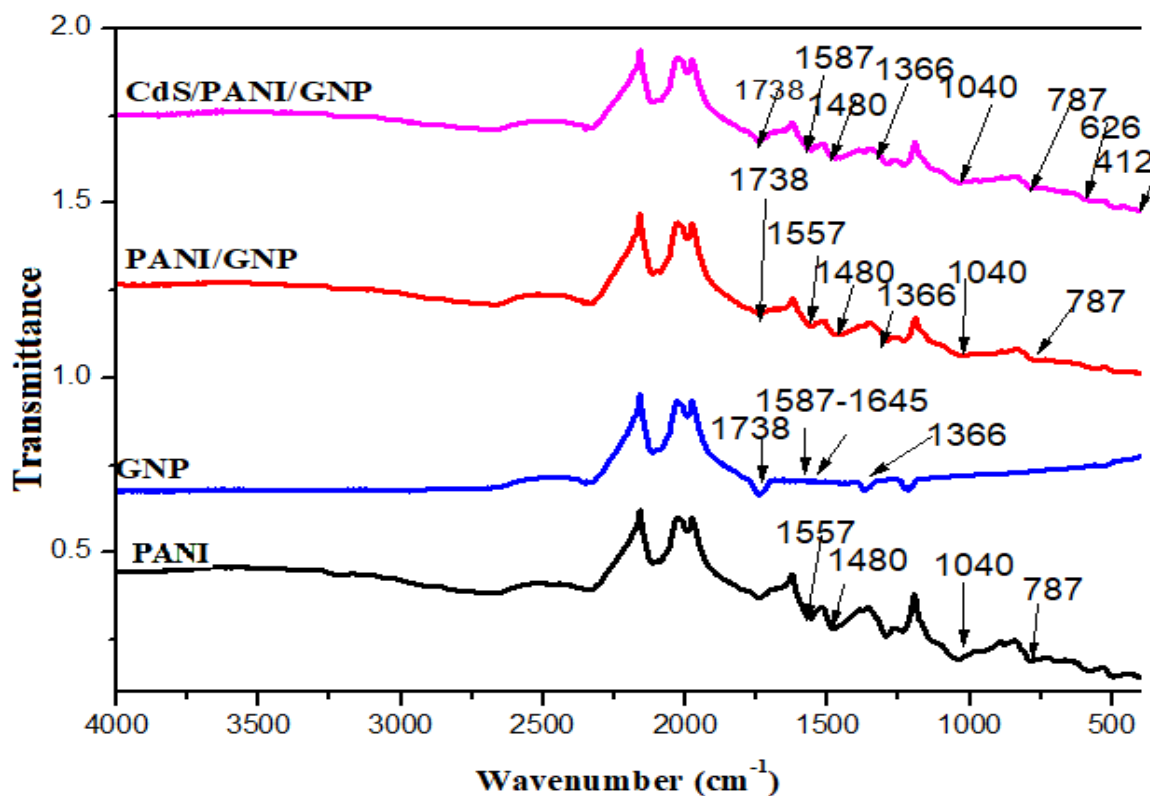


Fig.3.2 FTIR spectra of PANI, GNP, PANI/GNP and CdS/GNP/PANI synthesized by hydrothermal method.

Cyclic voltammetry

3.3 Cyclic voltammetry of Polyaniline

Cyclic voltammetry of polyaniline was performed in order to check its electrochemical and capacitive behavior in the potential range of -0.1 to 0.9 V in 1M aqueous sulfuric acid solution. The cyclic voltammetry of polyaniline shows three pairs characteristic peaks which are due to the redox reactions of polyaniline. These three pairs of peaks are **a/a'**, **b/b'** and **c/c'** can be seen in voltammogram as shown in Fig.3.3. The first peak **a/a'** is for the reversible reaction of leucoemeraldine into emeraldine. The second peak **b/b'** is due to the by-products and intermediates of hydroquinone/ benzoquinone. The third peak **c/c'** is for the reversible conversion of emeraldine into pernigraniline^{27a}.

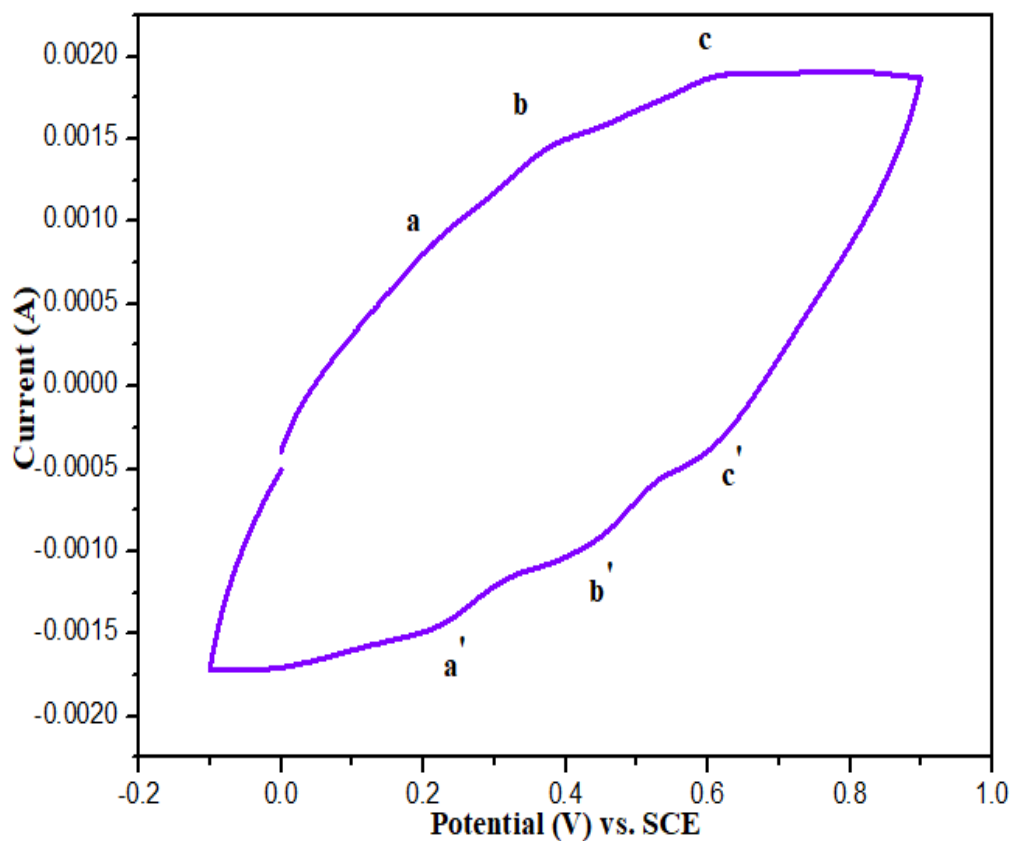


Fig.3.3 Cyclic voltammogram of polyaniline coated on GCE at 50mVs^{-1} in $1\text{M H}_2\text{SO}_4$ as a supporting electrolyte.

The cyclic voltammetry of polyaniline was also carried out at various scan rates as shown in Fig.3.4. The successive increase in the area in the CV loop with the increase in scan rate clearly indicates a linear relationship of scan rate and capacitance. At all scan rates the three reversible peaks survive.

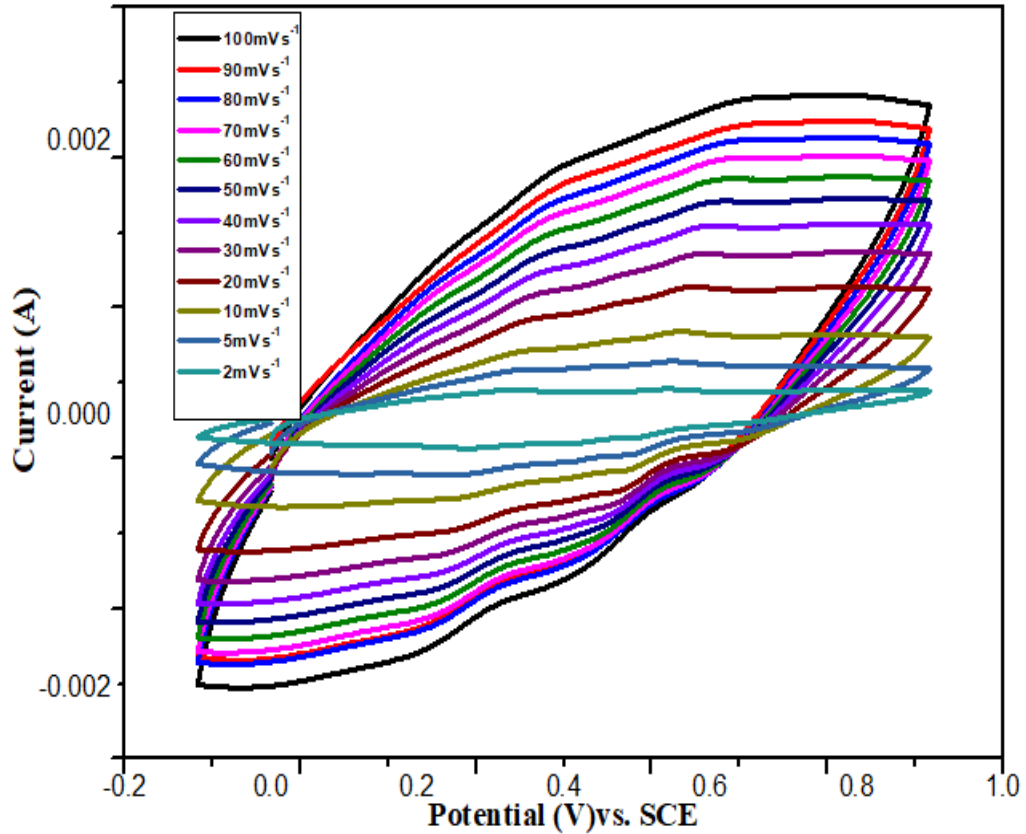


Fig.3.4 CVs of PANI coated on GCE in 1M H₂SO₄ as a supporting electrolyte at different scan rates.

3.3.1 Specific capacitance of polyaniline at various scan rates

The specific capacitance of polyaniline was calculated using Eq.1.8 in which IdV is the volumetric charge which comes from the integration of the CV curve. Potential window is 1 V and active mass of the electrode material is 0.1 mg. The Fig.3.5 shows the specific capacitance of polyaniline at different scan rates. It is clear that with the increase of scan rate the specific capacitance decreases. This is because at lower scan rate the electrolyte molecules have enough time to in order to penetrate into the pores of electrode material more properly and thus make larger surface contact and resulting into the high specific capacitance. In other words we it can be said that at higher scan rate the Ohmic resistance of the electrolyte migration increases in the pores of electrode material which results in smaller specific capacitance⁵⁷.

The Fig.3.5 shows the specific capacitance of polyaniline. The specific capacitance varies between 263F/g and 105F/g for corresponding scan rate range of 2mVs⁻¹ to

at 100 mVs^{-1} respectively. The polyaniline shows highest specific capacitance of 263.07 F/g at 2 mVs^{-1} . The variation of specific capacitance with scan rate is not exactly linear but very much close to it particularly for the intermediate values.

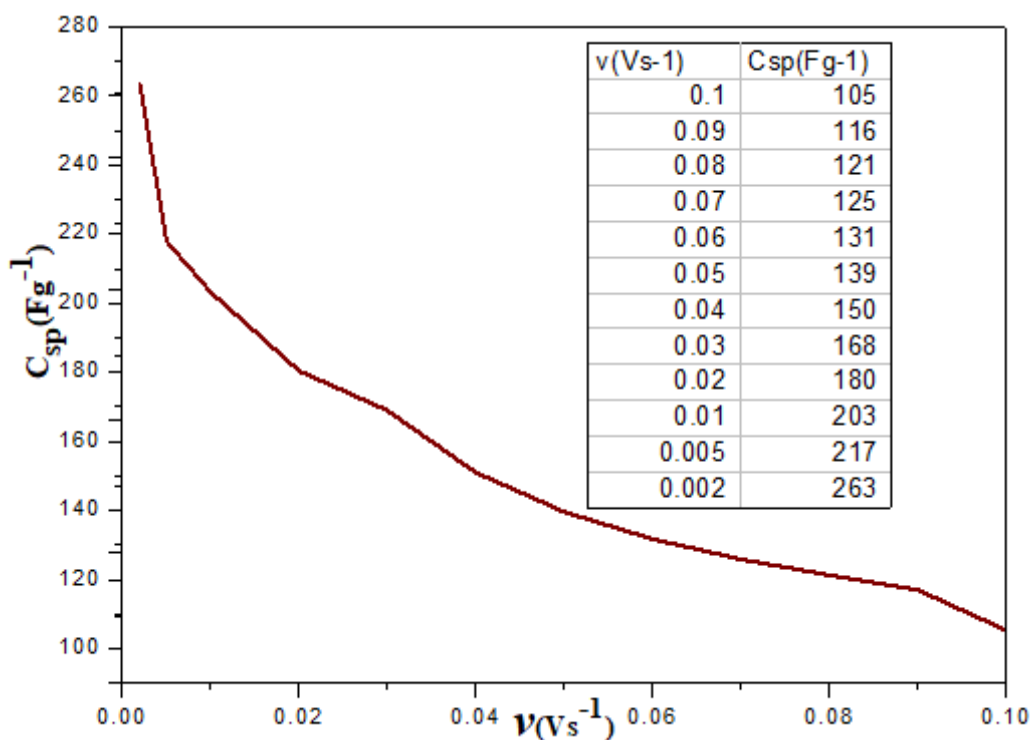


Fig.3.5 specific capacitance of polyaniline at various scan rates

3.3.2 Energy density calculation of polyaniline at various scan rates

Energy density of polyaniline was calculated using Eq. 1.14. polyaniline shows energy density of 36 Wh/kg , 30 Wh/kg , 28 Wh/kg , 25 Wh/kg , 23.45 Wh/kg , 19 Wh/kg and 14 Wh/kg at 2 mVs^{-1} , 5 mVs^{-1} , 10 mVs^{-1} , 20 mVs^{-1} , 30 mVs^{-1} , 50 mVs^{-1} and at 100 mVs^{-1} respectively. The values are following the same trend as was observed in the case of specific capacitance as expected. The higher energy density at low scan rate indicates the time required for the capability of the material to possess the capacitance per unit amount of the material.

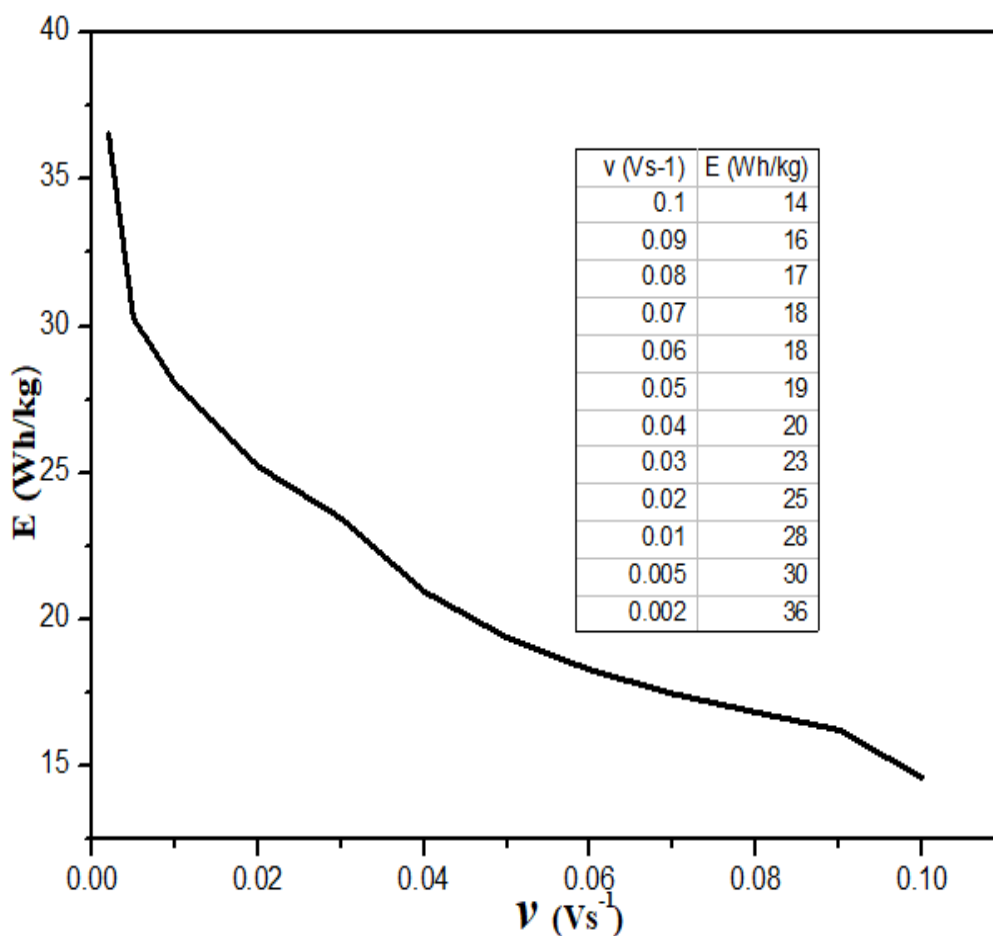


Fig 3.6 Energy density of polyaniline at different scan rate

3.4 Cyclic voltammetry of GNP/PANI

The cyclic voltammetry of this binary composite of GNP and polyaniline was performed in potential range of -0.1 to 0.9 V in 1M aqueous sulfuric acid solution employing three electrode configurations. Again the three pairs of reversible redox peaks were observed. These peaks become more prominent by the introduction of GNP. Fig.3.7 shows the cyclic voltammetry at 50mVs^{-1} . This cyclic voltammogram slightly looks rectangular in shape which is due to the incorporation of GNP into polyaniline because GNP has electrical double capacitance and such capacitance have rectangular cyclic voltammogram without any oxidation reduction peaks (which are usually present in pseudocapacitive materials like polyaniline transition metal oxides).

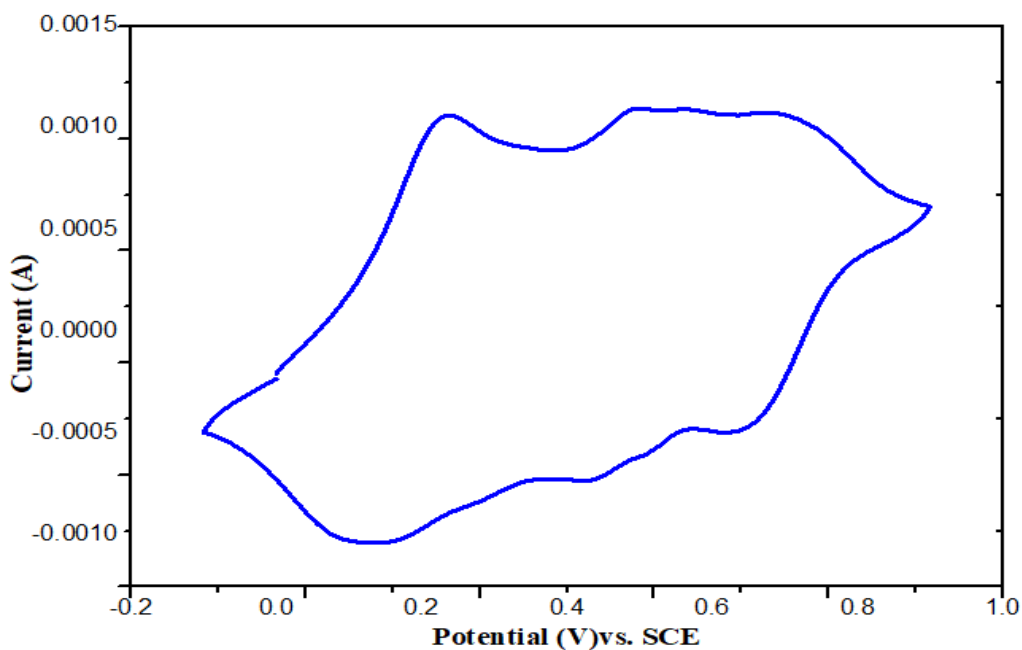


Fig.3.7 Cyclic voltammetry of GNP/PANI composite coated on GCE in 1M H₂SO₄ as a supporting electrolyte at 50mVs⁻¹.

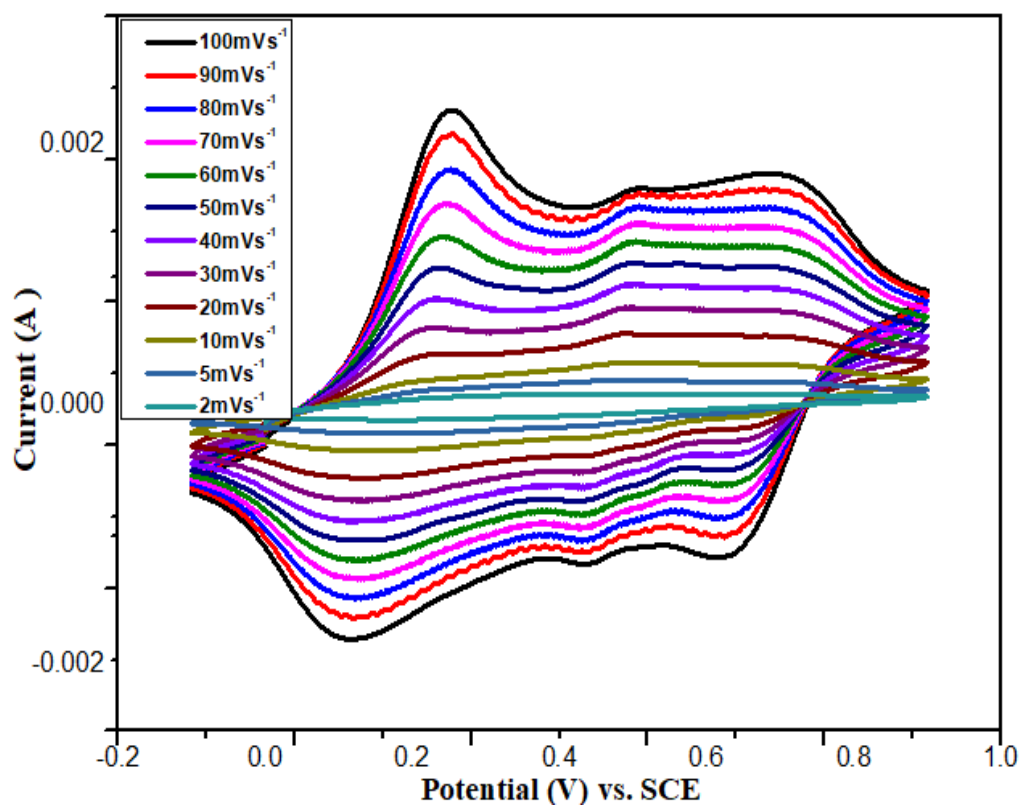


Fig.3.8 CVs GNP/PANI composite coated on GCE in 1M H₂SO₄ as a supporting electrolyte at different scan rates.

3.4.1 Specific capacitance and energy density of GNP/PANI

The specific capacitance of this binary composite was calculated in the same way as mentioned for polyaniline. The Fig.3.9 shows the specific capacitance of 540 F/g at 2mVs^{-1} , the highest value at the lowest scan rate. The rest of the values are given in the inset table of the Fig. 3.9. The specific capacitance of this composite is higher than the polyaniline about 100 times because here GNP also contributes into the capacitance because of its EDL capacitance while polyaniline store charges due to pseudocapitance. Energy density of GNP/PANI was calculated using Eq. 1.14. GNP/PANI shows higher energy density values as given in the Fig. 3.10. The higher capacitance and higher energy density values are clearly depicting the role of GNP. To our understanding it appears the higher conductivity, small amount with large surface area of GNP induced this improvement.

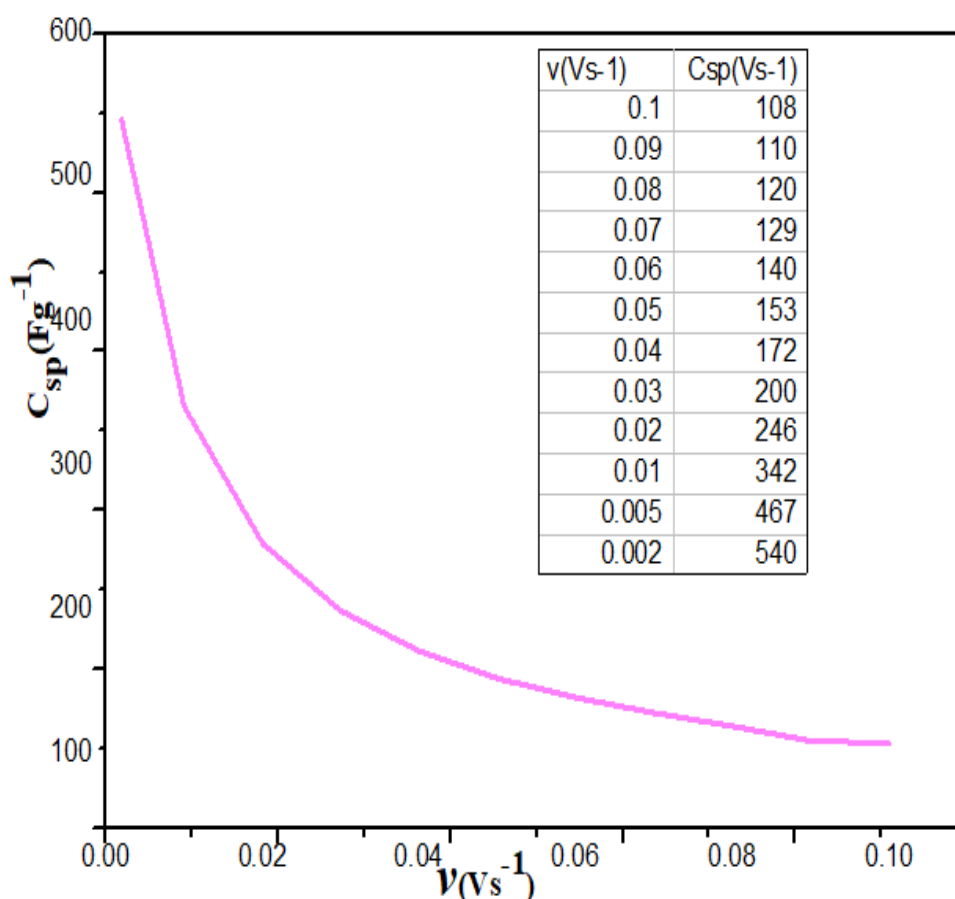


Fig.3.9 Specific capacitance of GNP/PANI at various scan rates.

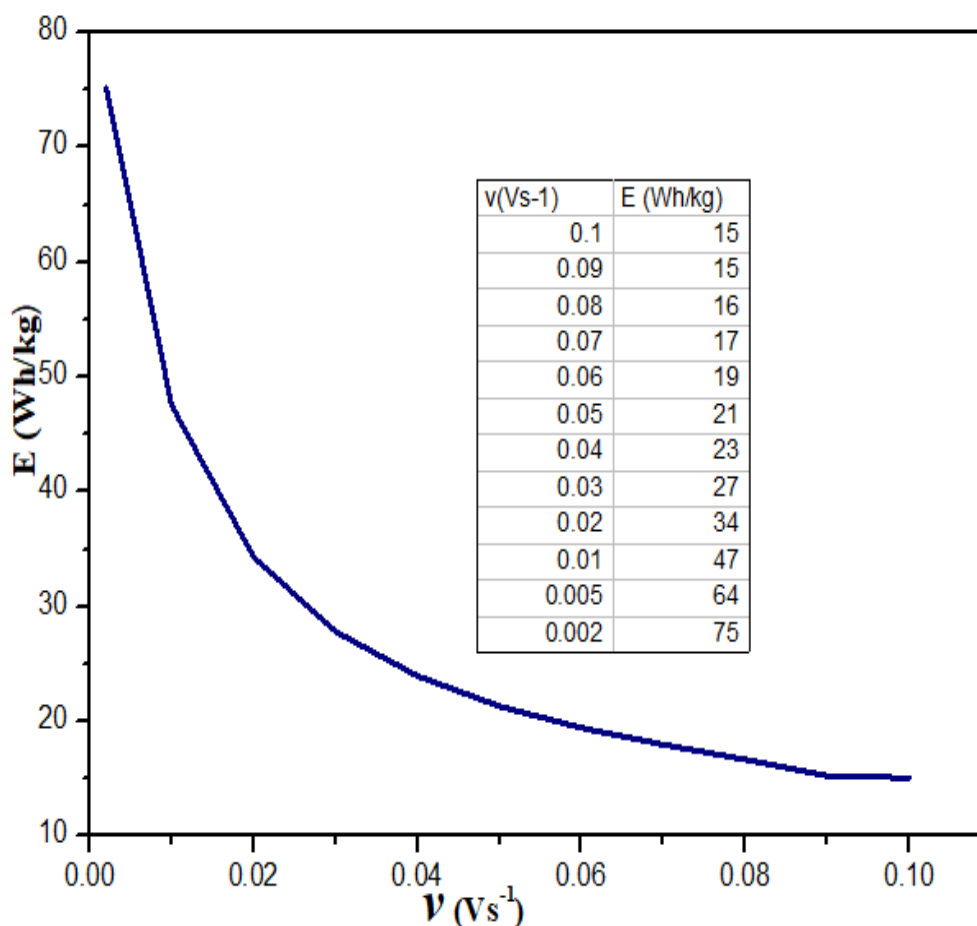


Fig.3.10Energy density of GNP/PANI at various scan rate.

3.5 Cyclic voltammetry of CdS/GNP/PANI

The cyclic voltammetry of the ternary composite was performed in 1M H₂SO₄ in the potential range from -0.1 to 0.9 V Fig.3.11 shows the cyclic voltammogram of the ternary composite. The obtained non-rectangular voltammogram shows the pseudocapacitive contribution of polyaniline to entire capacitance. In this voltammogram the three redox reversible pairs are due to the polyaniline conversion into other forms. Though the redox waves are not very sharp but the humps can easily be differentiated from each other. The three waves correspond to the sequential electron transfer processes of PANI as reported elsewhere^{27a}. Fig.3.12 shows the cyclic voltammogram at different scan rate. The increased capacitive current with the increase in scan rate is immediate proof of the higher capacitive ability of the material, however, the specific capacitance will give the actual ability of the material for charge storage.

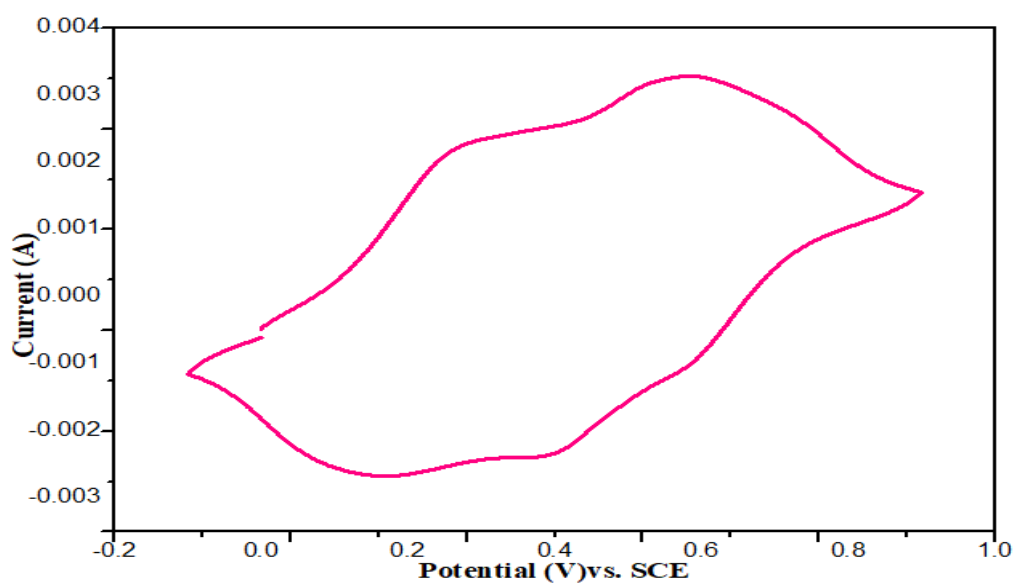


Fig.3.11 Cyclic voltammetry of CdS/GNP/PANI composite coated on GCE in 1M H₂SO₄ as a supporting electrolyte at 50mVs⁻¹.

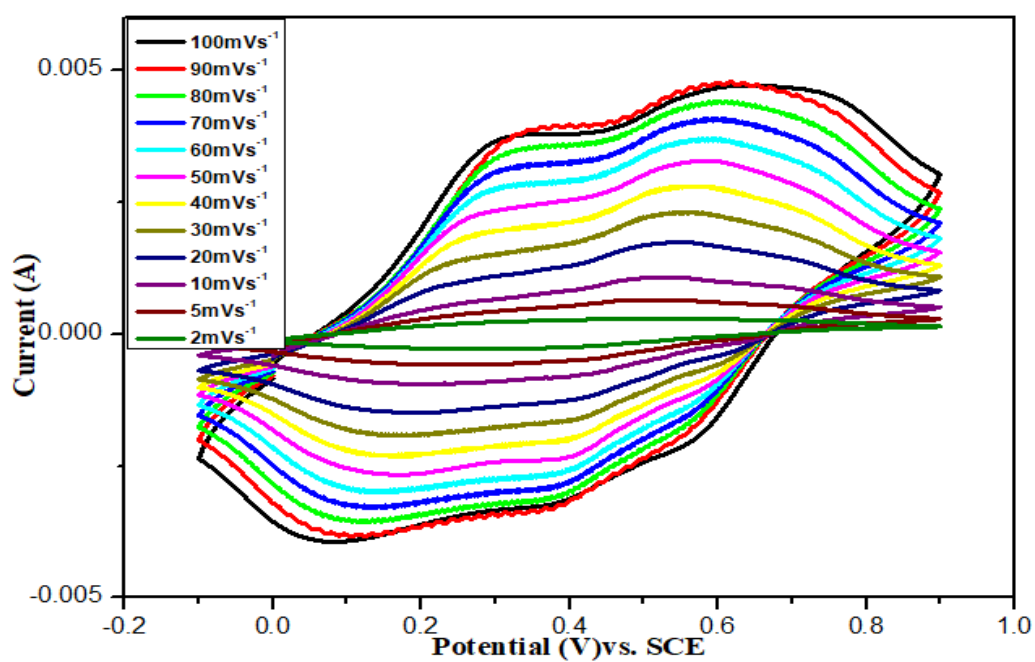


Fig.3.12 CVs of CdS/GNP/PANI composite coated on GCE in 1M H₂SO₄ as a supporting electrolyte at various scan rates.

3.5.1 Specific capacitance energy density of CdS/GNP/PANI

The specific capacitance of this ternary composite of CdS/GNP/PANI was calculated in the same way as mentioned for polyaniline. The Fig.3.13 shows the specific capacitance varying from 713 F/g to 234F/g for the selected range of scan rate i.e. from 2mVs^{-1} to 100mVs^{-1} .

The specific capacitance of ternary composite is 713 at 2mVs^{-1} which is higher than the polyaniline and polyaniline graphene nanoplatelets composite. The introduction of cadmium sulfide nanoparticles into GNP/PANI composite increases the capacitance about 32%. Similarly, the corresponding data of the energy density are given for the CdS/GNP/PANI having values of 99Wh/kg to 32Wh/kg for the scan rate of 2mVs^{-1} to 100mVs^{-1} as shown in Fig.3.14.

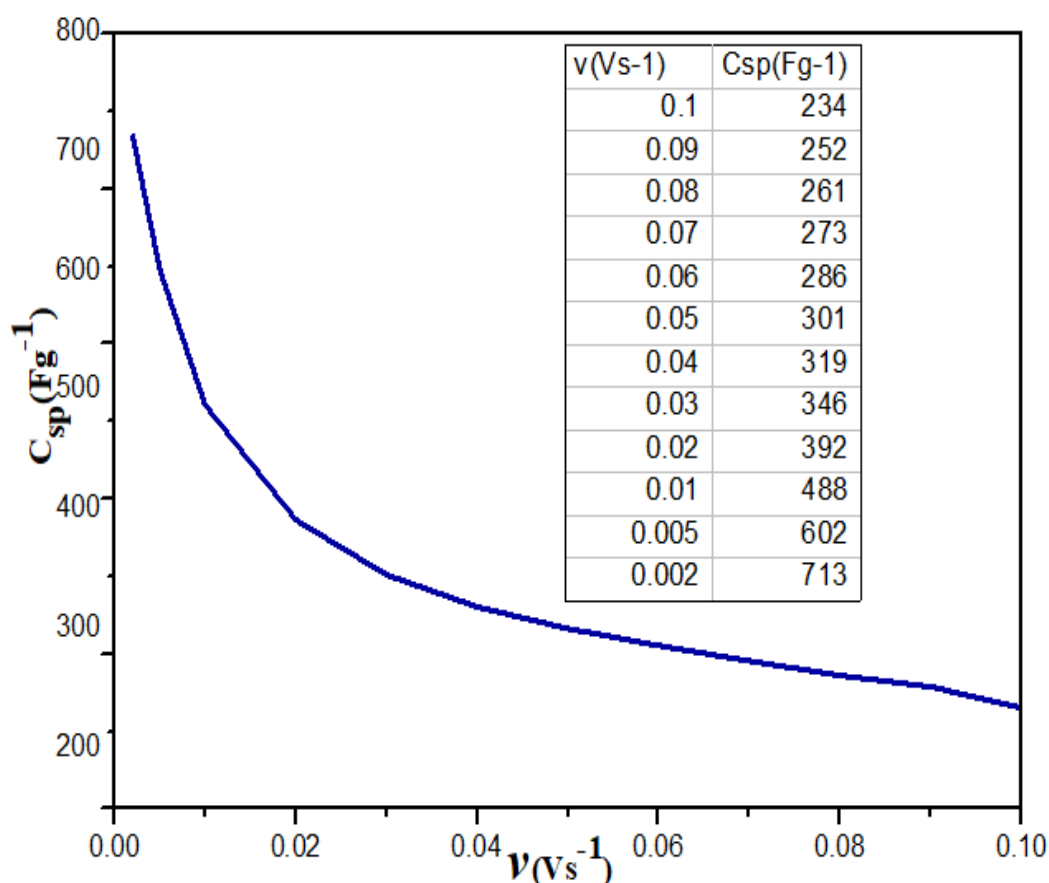


Fig.3.13 Specific capacitance of CdS/GNP/PANI at various scan rates.

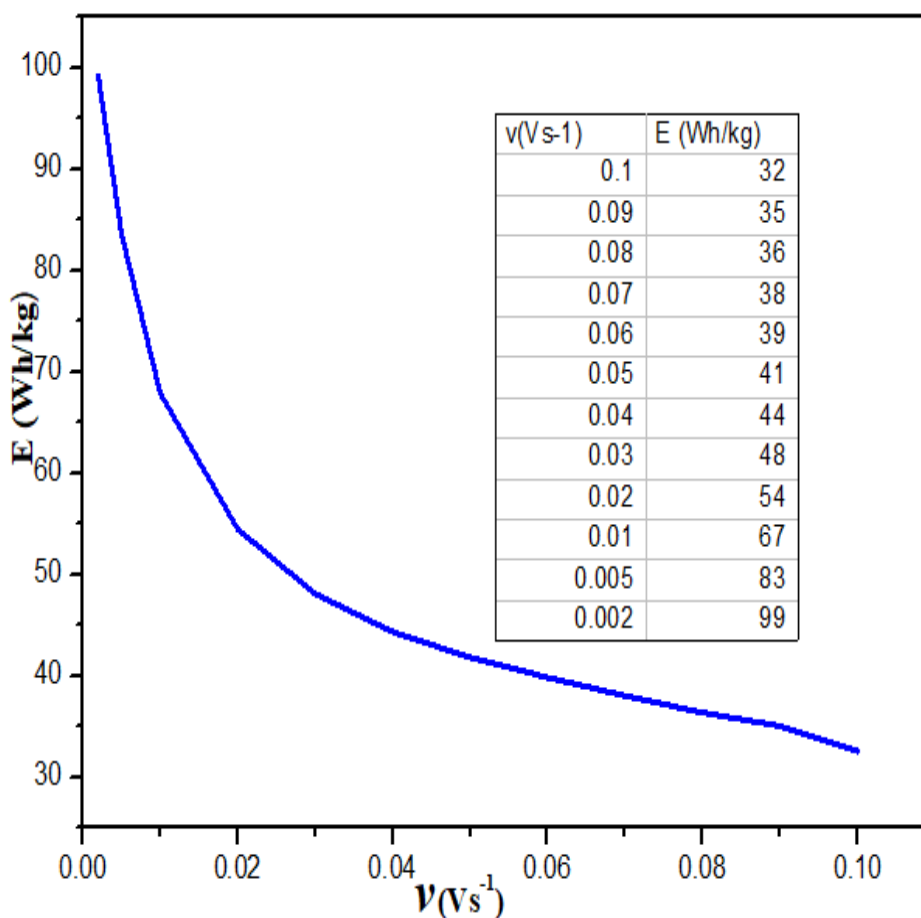


Fig 3.14 Energy density of CdS/GNP/PANI at various scan rates.

3.6 Comparison of the CV of the PANI, GNP/PANI and CdS/GNP/PANI

The CV of these three electrode materials was compared at 50mVs^{-1} and 100mVs^{-1} . It is clear from the shown Fig.3.15 and Fig.3.16 that ternary composite has higher current than polyaniline and GNP/PANI. The cyclic voltammogram of the ternary composite results in broader voltammogram because cadmium sulfide also contributes into capacitance. The marked increase in the capacitive current but not in the electron transfer current clearly indicates the charge storage ability of the material which was complemented later by the specific capacitance data.

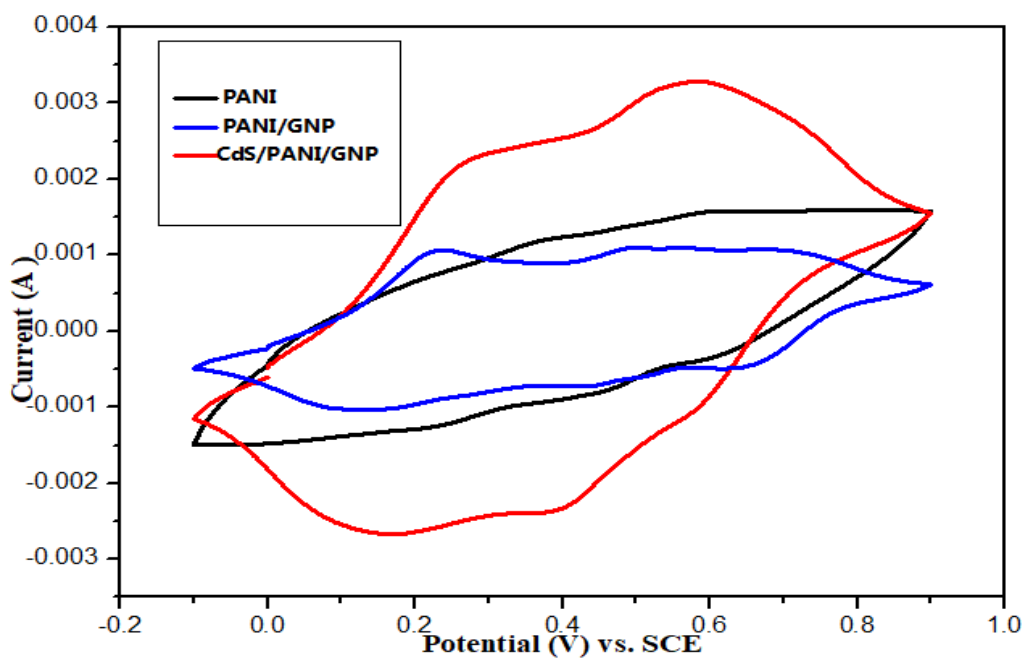


Fig.3.15 Comparison of CV response of PANI, PANI/GNP and CdS/GNP/PANI CV coated on GCE in 1M H₂SO₄ as a supporting electrolyte at 50mVs⁻¹.

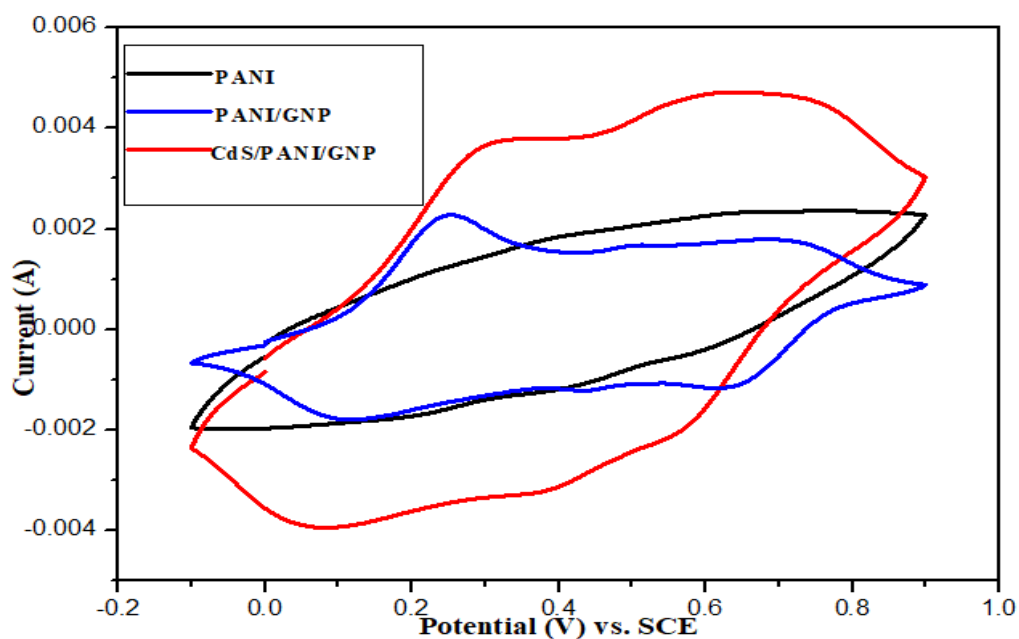


Fig.3.16 Comparison of CV response of PANI, PANI/GNP and CdS/GNP/PANICV coated on GCE in 1M H₂SO₄ as a supporting electrolyte at 100mVs⁻¹.

3.7 Comparison of the specific capacitance and energy density of PANI, GNP/PANI and CdS/GNP/PANI

Fig.3.17 shows the comparison of the polyaniline GNP/PANI and CdS/GNP/PANI. It is clear that the ternary composite has higher specific capacitance at all scan rates. This is due the good synergistic effect of cadmium sulfide with the polyaniline and graphene nanoplatelets resulting in high specific capacitance. The larger specific capacitance of ternary composite also reveals the π - π interaction and combined effect of the individual constituents which are present in the ternary composite. Polyaniline shows specific capacitance of 263Fg^{-1} with the introduction of GNP the specific capacitance increase to 540Fg^{-1} which shows almost 100 times increase. This is because now GNP stores charges because of its electrical double layer capacitance. When GNP/PANI was further modified with cadmium sulfide it shows specific capacitance of 713Fg^{-1} which is 36 times increase. Fig.3.18 shows the comparison of energy density of GNP/PANI and CdS/GNP/PANI.

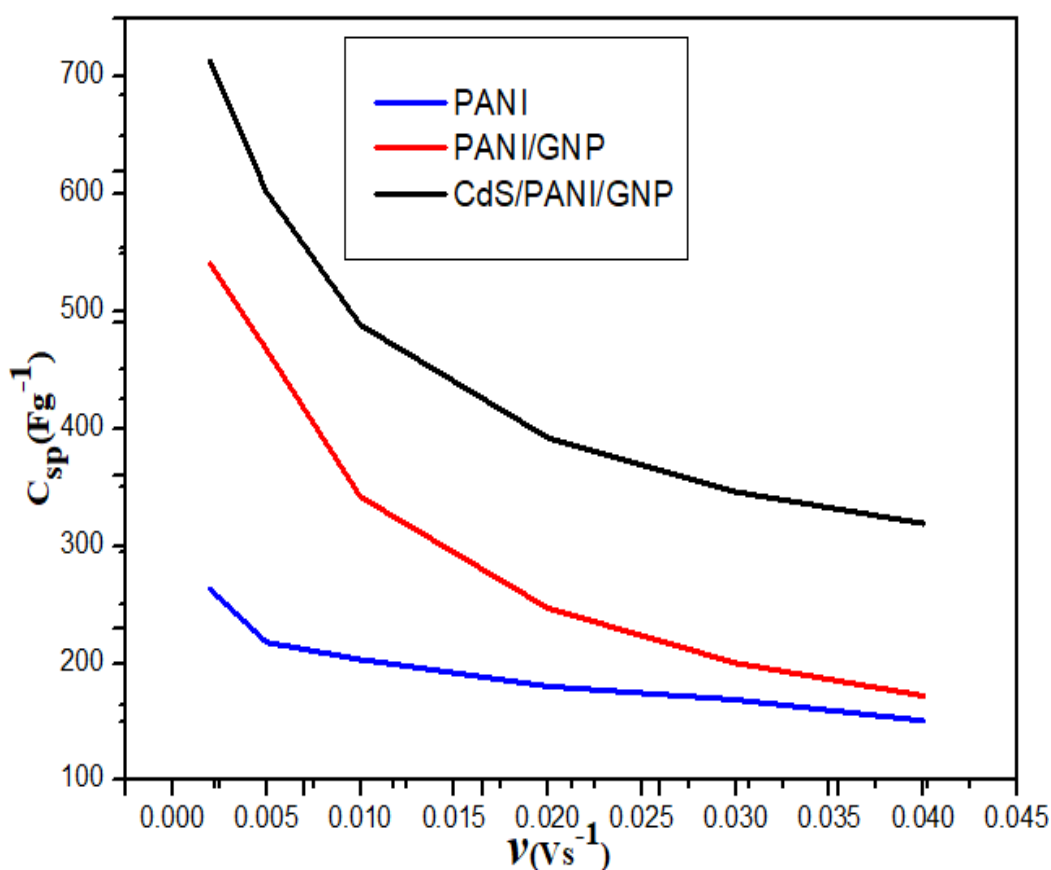


Fig.3.17 Comparison of specific capacitance of PANI, GNP/PANI and CdS/GNP/PANI.

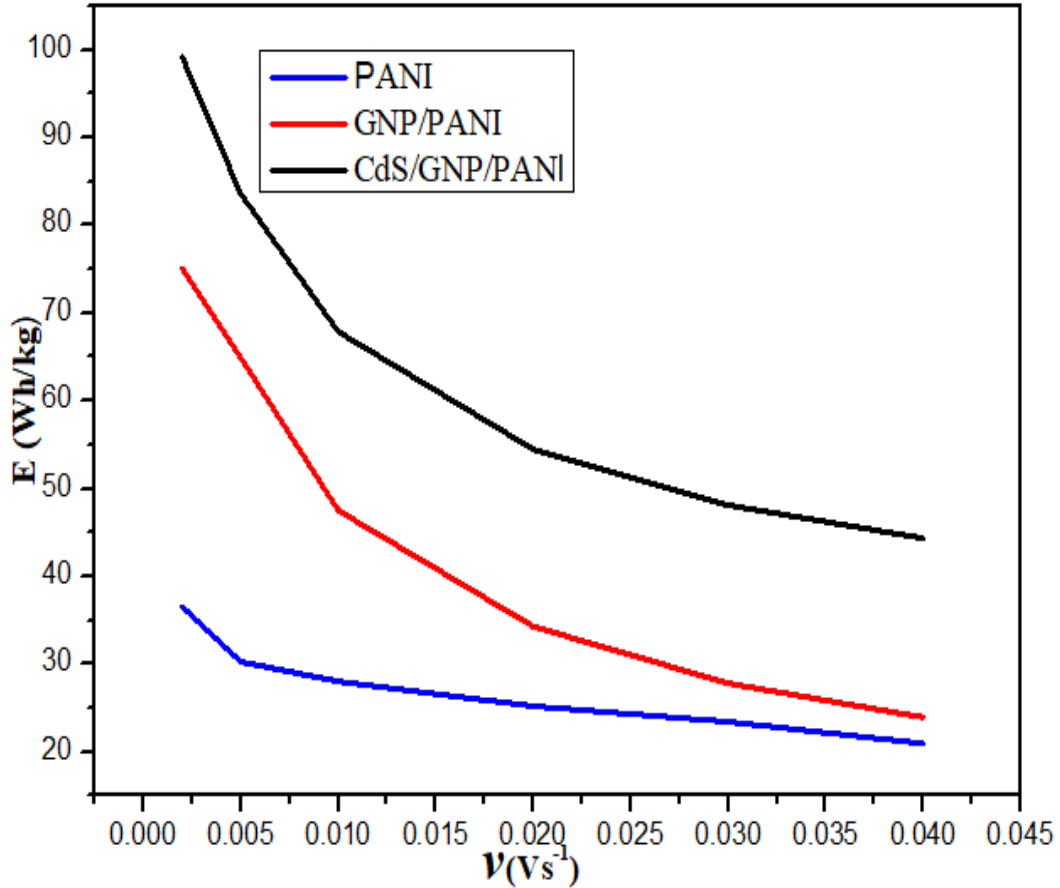


Fig.3.18 Comparison of energy density of PANI, GNP/PANI and CdS/GNP/PANI.

3.8 Stability of the CdS/GNP/PANI

The stability of the ternary composite of CdS/GNP/PANI was checked in 1M H_2SO_4 in the potential window of -0.1 to 0.9 V for 1000 cycles at $100mVs^{-1}$ in a three electrode configuration. From the Fig.3.19 it is obvious that specific capacitance increases at the start of the cycles and then slightly decreases. After 1000th cycles still 84% of its specific capacitance was maintained as shown in Fig.3.20. This is because of good combined effect of GNP with polyaniline. Polyaniline if used alone then it has problem of volumetric shrinkage. In this volumetric shrinkage there is ejection of doped ions from the polyaniline thus resulting in low conductivity of polyaniline and consequently low specific capacitance of polyaniline.

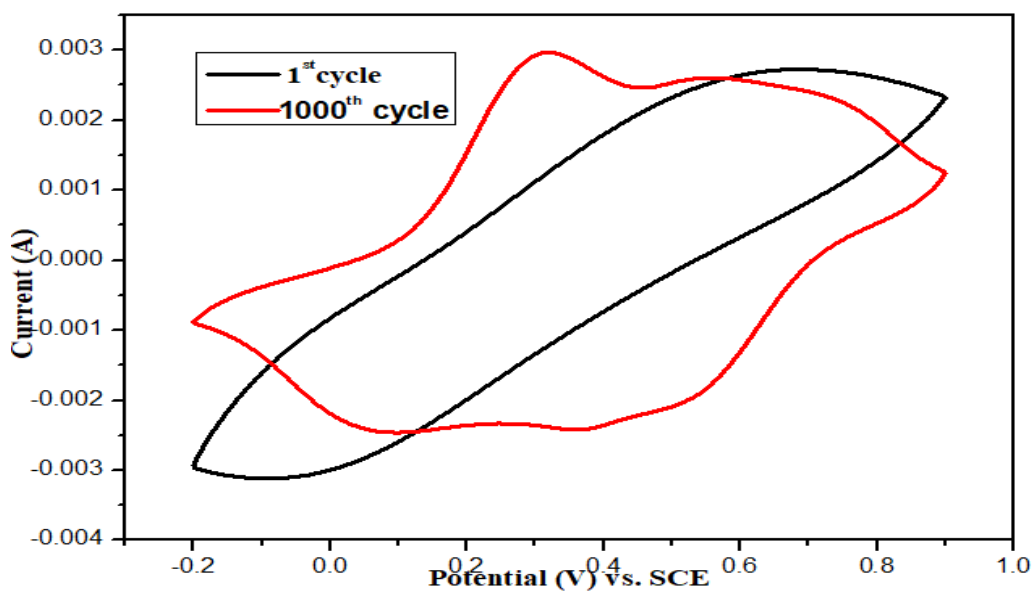


Fig.3.19 Stability of CdS/GNP/PANI coated on GCE in 1M H₂SO₄ as a supporting electrolyte at 100mVs⁻¹ first and 1000th cycle.

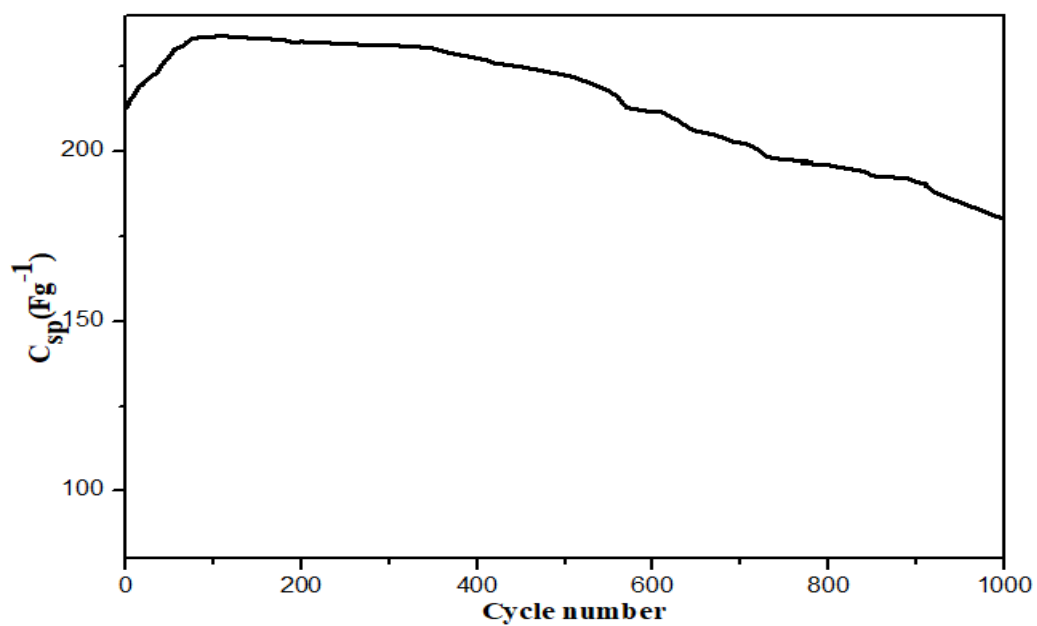


Fig.3.20 Specific capacitance of CdS/PANI/GNP vs cycle no.

3.9 Nature of process-statistical analysis

The peak current (i) in the CV and scan rate (v) at which CV is performed obeys power law which is given below as⁵⁸

$$I = av^b \quad (3.1)$$

Taking log of Eq. 3.2

$$\log(i) = b\log(v) + \log a \quad (3.2)$$

Here a and b are variables. The value of b can be found from the slope of $\log(i)$ vs. $\log(v)$ plot. The value of b tells us about the nature of electrochemical process. If the value of $b=0.5$ it means it is a diffusion controlled process and if the value of $b=1$ it means the process is capacitance controlled process⁵⁸. On application of applied Eq. 3.2 to the CV data of the ternary composite of CdS/GNP/PANI and plot the log of anodic peak current vs log of scan rate, following results are obtained.

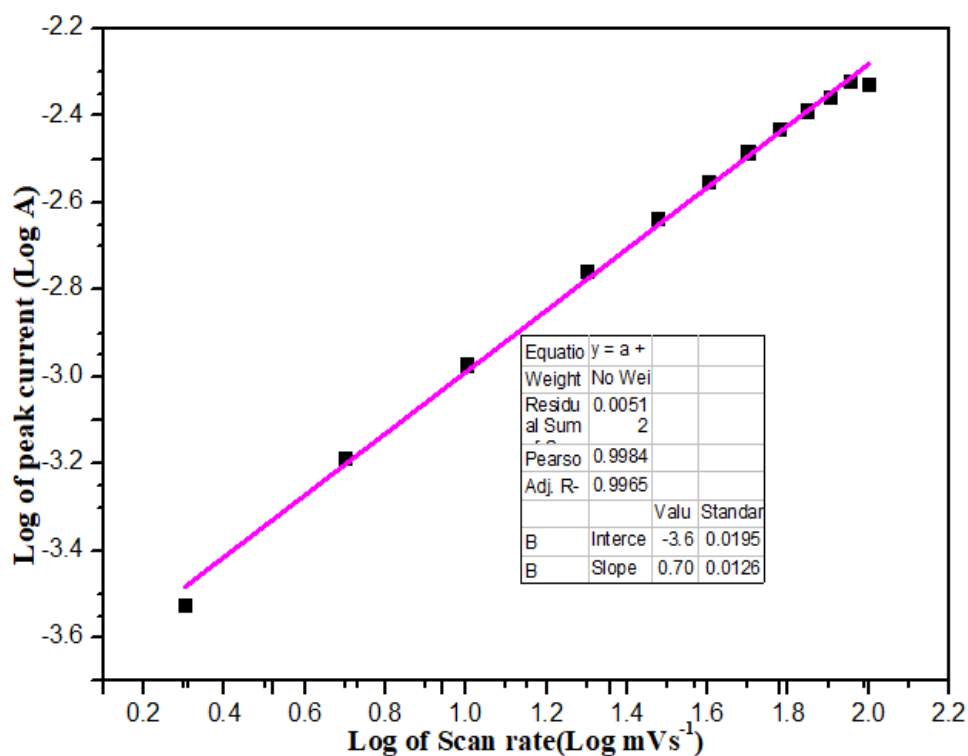


Fig.3.21 Statistical analysis of electrochemical process.

The value of slope was 0.70 showing that the electrochemical process of the ternary composite is both diffusion controlled and capacitive controlled. The capacitive nature of the ternary composite is due to the GNP and CdS.

3.10 Conclusions

In this work composite of cadmium sulfide and polyaniline was successfully synthesized which is further modified by graphene nanoplatelets. The synthesis procedure involved the formation of CdS/GNP composite by hydrothermal reaction followed by *insitu* polymerization of aniline. This ternary composite of CdS/GNP/PANI was confirmed by XRD and FTIR studies. In electrochemical characterization cyclic voltammetry was employed to identify the faradic and non-faradic processes in the synthesized material. The ternary composite shows a high specific capacitance of 713 Fg^{-1} at 2mVs^{-1} and energy density of 99 Whkg^{-1} . Stability of this composite was checked for 1000 consecutive cycles and it showed about 82% retention of its specific capacitance.

These references are corrected in separate file according to farman, and he said at the time of printing he will attach that file which he have corrected.

REFERENCES

1. Conway, B. E., *Electrochemical supercapacitors: scientific fundamentals and technological applications*. Springer Science & Business Media: 2013.
2. Linden, D.; Reddy, T. B., *Handbook of Batteries*. 3rd. *McGraw-Hill* **2002**.
3. Zhu, Y.; Murali, S.; Stoller, M. D.; Ganesh, K.; Cai, W.; Ferreira, P. J.; Pirkle, A.; Wallace, R. M.; Cyhosh, K. A.; Thommes, M., Carbon-based supercapacitors produced by activation of graphene. *Science* **2011**,332 (6037), 1537-1541.
4. Shukla, A.; Sampath, S.; Vijayamohan, K., Electrochemical supercapacitors: Energy storage beyond batteries. *CURRENT SCIENCE-BANGALORE*- **2000**,79 (12), 1656-1661.
5. Kate, R. S.; Khalate, S. A.; Deokate, R. J., Overview of nanostructured metal oxides and pure nickel oxide (NiO) electrodes for supercapacitors: a review. *Journal of Alloys and Compounds* **2018**,734, 89-111.
6. Saha, S.; Samanta, P.; Murmu, N. C.; Kuila, T., A review on the heterostructure nanomaterials for supercapacitor application. *Journal of Energy Storage* **2018**,17, 181-202.
7. Yoo, J. J.; Balakrishnan, K.; Huang, J.; Meunier, V.; Sumpter, B. G.; Srivastava, A.; Conway, M.; Mohana Reddy, A. L.; Yu, J.; Vajtai, R., Ultrathin planar graphene supercapacitors. *Nano letters* **2011**,11 (4), 1423-1427.
8. Xie, J.; Yang, P.; Wang, Y.; Qi, T.; Lei, Y.; Li, C. M., Puzzles and confusions in supercapacitor and battery: Theory and solutions. *Journal of Power Sources* **2018**,401, 213-223.
9. Huang, M.; Li, F.; Dong, F.; Zhang, Y. X.; Zhang, L. L., MnO₂-based nanostructures for high-performance supercapacitors. *Journal of Materials Chemistry A* **2015**,3 (43), 21380-21423.
10. Conway, B.; Birss, V.; Wojtowicz, J., The role and utilization of pseudocapacitance for energy storage by supercapacitors. *Journal of Power Sources* **1997**,66 (1-2), 1-14.
11. (a) Chen, G. Z., Supercapacitor and supercapattery as emerging electrochemical energy stores. *International Materials Reviews* **2017**,62 (4), 173-202;(b) Li, J.; O'Shea, J.; Hou, X.; Chen, G. Z., Faradaic processes beyond Nernst's law: density functional theory assisted modelling of partial electron delocalisation and pseudocapacitance in graphene oxides. *Chemical Communications* **2017**,53 (75), 10414-10417.
12. Zhi, M.; Xiang, C.; Li, J.; Li, M.; Wu, N., Nanostructured carbon-metal oxide composite electrodes for supercapacitors: a review. *Nanoscale* **2013**,5 (1), 72-88.
13. Dubal, D. P.; Ayyad, O.; Ruiz, V.; Gomez-Romero, P., Hybrid energy storage: the merging of battery and supercapacitor chemistries. *Chemical Society Reviews* **2015**,44 (7), 1777-1790.
14. Wang, G.; Zhang, L.; Zhang, J., A review of electrode materials for electrochemical supercapacitors. *Chemical Society Reviews* **2012**,41 (2), 797-828.
15. Dang, Y.-Q.; Ren, S.-Z.; Liu, G.; Cai, J.; Zhang, Y.; Qiu, J., Electrochemical and capacitive properties of carbon dots/reduced graphene oxide supercapacitors. *Nanomaterials* **2016**,6 (11), 212.
16. Klumpp, C.; Kostarelos, K.; Prato, M.; Bianco, A., Functionalized carbon nanotubes as emerging nanovectors for the delivery of therapeutics. *Biochimica et Biophysica Acta (BBA)- Biomembranes* **2006**,1758 (3), 404-412.
17. Pandey, P.; Dahiya, M., Carbon nanotubes: Types, methods of preparation and applications. *Carbon* **2016**,1 (4).

18. (a) Farzana, R.; Rajarao, R.; Bhat, B. R.; Sahajwalla, V., Performance of an activated carbon supercapacitor electrode synthesised from waste Compact Discs (CDs). *Journal of Industrial and Engineering Chemistry* **2018**;(b) Rivera-Utrilla, J.; Sánchez-Polo, M.; Gómez-Serrano, V.; Alvarez, P.; Alvim-Ferraz, M.; Dias, J., Activated carbon modifications to enhance its water treatment applications. An overview. *Journal of hazardous materials* **2011**,187 (1-3), 1-23.
19. Allen, M. J.; Tung, V. C.; Kaner, R. B., Honeycomb carbon: a review of graphene. *Chemical reviews* **2009**,110 (1), 132-145.
20. Ke, Q.; Wang, J., Graphene-based materials for supercapacitor electrodes—A review. *Journal of Materiomics* **2016**,2 (1), 37-54.
21. Rowley-Neale, S. J.; Randviir, E. P.; Dena, A. S. A.; Banks, C. E., An overview of recent applications of reduced graphene oxide as a basis of electroanalytical sensing platforms. *Applied Materials Today* **2018**,10, 218-226.
22. Yang, H.; Kannappan, S.; Pandian, A. S.; Jang, J.-H.; Lee, Y. S.; Lu, W., Graphene supercapacitor with both high power and energy density. *Nanotechnology* **2017**,28 (44), 445401.
23. (a) Wang, H.; Hao, Q.; Yang, X.; Lu, L.; Wang, X., A nanostructured graphene/polyaniline hybrid material for supercapacitors. *Nanoscale* **2010**,2 (10), 2164-2170;(b) Wu, Z.-S.; Zhou, G.; Yin, L.-C.; Ren, W.; Li, F.; Cheng, H.-M., Graphene/metal oxide composite electrode materials for energy storage. *Nano Energy* **2012**,1 (1), 107-131.
24. Krishnamoorthy, K.; Pazhamalai, P.; Kim, S. J., Ruthenium sulfide nanoparticles as a new pseudocapacitive material for supercapacitor. *Electrochimica Acta* **2017**,227, 85-94.
25. Zhang, Y.; Feng, H.; Wu, X.; Wang, L.; Zhang, A.; Xia, T.; Dong, H.; Li, X.; Zhang, L., Progress of electrochemical capacitor electrode materials: A review. *International journal of hydrogen energy* **2009**,34 (11), 4889-4899.
26. Rudge, A.; Davey, J.; Raistrick, I.; Gottesfeld, S.; Ferraris, J. P., Conducting polymers as active materials in electrochemical capacitors. *Journal of Power Sources* **1994**,47 (1-2), 89-107.
27. (a) Li, H.; Wang, J.; Chu, Q.; Wang, Z.; Zhang, F.; Wang, S., Theoretical and experimental specific capacitance of polyaniline in sulfuric acid. *Journal of Power Sources* **2009**,190 (2), 578-586;(b) Eftekhari, A.; Li, L.; Yang, Y., Polyaniline supercapacitors. *Journal of Power Sources* **2017**,347, 86-107.
28. Adhikari, A. D.; Oraon, R.; Tiwari, S. K.; Saren, P.; Lee, J. H.; Kim, N. H.; Nayak, G. C., CdS-CoFe₂O₄@ Reduced Graphene Oxide Nanohybrid: An Excellent Electrode Material for Supercapacitor Applications. *Industrial & Engineering Chemistry Research* **2018**,57 (5), 1350-1360.
29. (a) Ohno, H.; Fukumoto, K., Progress in ionic liquids for electrochemical reaction matrices. *Electrochemistry* **2008**,76 (1), 16-23;(b) Galiński, M.; Lewandowski, A.; Stępnia, I., Ionic liquids as electrolytes. *Electrochimica acta* **2006**,51 (26), 5567-5580.
30. Bard, A.; Faulkner, L., *Electrochemical methods: fundamentals and applications*. 2001, Hoboken. NJ: John Wiley & Sons, Inc.
31. Chen, G. Z., Understanding supercapacitors based on nano-hybrid materials with interfacial conjugation. *Progress in Natural Science: Materials International* **2013**,23 (3), 245-255.
32. Moussa, M.; El-Kady, M. F.; Zhao, Z.; Majewski, P.; Ma, J., Recent progress and performance evaluation for polyaniline/graphene nanocomposites as supercapacitor electrodes. *Nanotechnology* **2016**,27 (44), 442001.
33. Xu, P.; Liu, J.; Yan, P.; Miao, C.; Ye, K.; Cheng, K.; Yin, J.; Cao, D.; Li, K.; Wang, G., Preparation of porous cadmium sulphide on nickel foam: a novel electrode material with excellent supercapacitor performance. *Journal of Materials Chemistry A* **2016**,4 (13), 4920-4928.
34. Nair, N.; Sankapal, B. R., Nested CdS@ HgS core-shell nanowires as supercapacitive Faradaic electrode through simple solution chemistry. *Nano-Structures & Nano-Objects* **2017**,10, 159-166.
35. Patil, D. S.; Pawar, S. A.; Shin, J. C., Core-shell structure of Co₃O₄@ CdS for high performance electrochemical supercapacitor. *Chemical Engineering Journal* **2018**,335, 693-702.
36. Chen, L.; Zuo, Y.; Zhang, Y.; Gao, Y., Cadmium sulfide anchored in three-dimensional graphite cage for high performance supercapacitors. *Applied Physics Letters* **2018**,112 (22), 223901.

37. Patil, D. S.; Pawar, S. A.; Shin, J. C., Alteration of Ag nanowires to Ag/Ag₂S nanowires@ CdS core-shell architectures for electrochemical supercapacitors. *Journal of Alloys and Compounds* **2018**,*768*, 1076-1082.
38. Arbizzani, C.; Mastragostino, M.; Meneghello, L., Polymer-based redox supercapacitors: A comparative study. *Electrochimica Acta* **1996**,*41* (1), 21-26.
39. Ryu, K. S.; Kim, K. M.; Park, N.-G.; Park, Y. J.; Chang, S. H., Symmetric redox supercapacitor with conducting polyaniline electrodes. *Journal of Power Sources* **2002**,*103* (2), 305-309.
40. Chen, W.-C.; Wen, T.-C.; Teng, H., Polyaniline-deposited porous carbon electrode for supercapacitor. *Electrochimica Acta* **2003**,*48* (6), 641-649.
41. Gupta, V.; Miura, N., High performance electrochemical supercapacitor from electrochemically synthesized nanostructured polyaniline. *Materials Letters* **2006**,*60* (12), 1466-1469.
42. Dhawale, D.; Vinu, A.; Lokhande, C., Stable nanostructured polyaniline electrode for supercapacitor application. *Electrochimica Acta* **2011**,*56* (25), 9482-9487.
43. Khdary, N. H.; Abdesalam, M. E.; Enany, G. E., Mesoporous polyaniline films for high performance supercapacitors. *Journal of The Electrochemical Society* **2014**,*161* (9), G63-G68.
44. Feng, X. M.; Li, R. M.; Ma, Y. W.; Chen, R. F.; Shi, N. E.; Fan, Q. L.; Huang, W., One-step electrochemical synthesis of graphene/polyaniline composite film and its applications. *Advanced Functional Materials* **2011**,*21* (15), 2989-2996.
45. Ma, B.; Zhou, X.; Bao, H.; Li, X.; Wang, G., Hierarchical composites of sulfonated graphene-supported vertically aligned polyaniline nanorods for high-performance supercapacitors. *Journal of Power Sources* **2012**,*215*, 36-42.
46. Yu, L.; Gan, M.; Ma, L.; Huang, H.; Hu, H.; Li, Y.; Tu, Y.; Ge, C.; Yang, F.; Yan, J., Facile synthesis of MnO₂/polyaniline nanorod arrays based on graphene and its electrochemical performance. *Synthetic Metals* **2014**,*198*, 167-174.
47. Das, A. K.; Karan, S. K.; Khatua, B., High energy density ternary composite electrode material based on polyaniline (PANI), molybdenum trioxide (MoO₃) and graphene nanoplatelets (GNP) prepared by sono-chemical method and their synergistic contributions in superior supercapacitive performance. *Electrochimica Acta* **2015**,*180*, 1-15.
48. Li, X.; Zhang, C.; Xin, S.; Yang, Z.; Li, Y.; Zhang, D.; Yao, P., Facile synthesis of MoS₂/reduced graphene oxide@ polyaniline for high-performance supercapacitors. *ACS applied materials & interfaces* **2016**,*8* (33), 21373-21380.
49. Purty, B.; Choudhary, R.; Biswas, A.; Udayabhanu, G., Potentially enlarged supercapacitive values for CdS-PPY decorated rGO nanocomposites as electrode materials. *Materials Chemistry and Physics* **2018**.
50. Cazes, J., *Analytical instrumentation handbook*. CRC Press: 2004.
51. Bertin, E. P., *Principles and practice of X-ray spectrometric analysis*. Springer Science & Business Media: 2012.
52. Skoog, D. A.; Holler, F. J.; Crouch, S. R., *Principles of instrumental analysis*. Cengage learning: 2017.
53. Xiang, Z.; Nan, J.; Deng, J.; Shi, Y.; Zhao, Y.; Zhang, B.; Xiang, X., Uniform CdS-decorated carbon microsheets with enhanced photocatalytic hydrogen evolution under visible-light irradiation. *Journal of Alloys and Compounds* **2019**,*770*, 886-895.
54. Al-Fahdi, T.; Al Marzouqi, F.; Kuvarega, A. T.; Mamba, B. B.; Al Kindy, S. M.; Kim, Y.; Selvaraj, R., Visible light active CdS@ TiO₂ core-shell nanostructures for the photodegradation of chlorophenols. *Journal of Photochemistry and Photobiology A: Chemistry* **2019**.
55. (a) Talbi, L.; Berouaken, M.; Khaldi, K.; Keffous, A.; Gabouze, N.; Trari, M.; Menari, H.; Belkacem, Y., Elaboration and characterization of electrochemically prepared H⁺-doped polyaniline/Au/a-SiC: H-based chemical sensor. *Journal of Solid State Electrochemistry* **2018**,*22* (4), 1123-1130;(b) Wang, R.; Han, M.; Zhao, Q.; Ren, Z.; Guo, X.; Xu, C.; Hu, N.; Lu, L., Hydrothermal

synthesis of nanostructured graphene/polyaniline composites as high-capacitance electrode materials for supercapacitors. *Scientific reports* **2017**,*7*, 44562.

56. (a) Habibi, M. H.; Rahmati, M. H., Fabrication and characterization of ZnO@ CdS core-shell nanostructure using acetate precursors: XRD, FESEM, DRS, FTIR studies and effects of cadmium ion concentration on band gap. *Spectrochimica Acta Part A: Molecular and Biomolecular Spectroscopy* **2014**,*133*, 13-18;(b) Wang, H.; Fang, P.; Chen, Z.; Wang, S., Synthesis and characterization of CdS/PVA nanocomposite films. *Applied Surface Science* **2007**,*253* (20), 8495-8499.

57. Mishra, N.; Shinde, S.; Vishwakarma, R.; Kadam, S.; Sharon, M.; Sharon, M. In *MWCNTs synthesized from waste polypropylene plastics and its application in super-capacitors*, AIP Conference Proceedings, AIP: 2013; pp 228-236.

58. Li, H.; Lang, J.; Lei, S.; Chen, J.; Wang, K.; Liu, L.; Zhang, T.; Liu, W.; Yan, X., A High-Performance Sodium-Ion Hybrid Capacitor Constructed by Metal–Organic Framework–Derived Anode and Cathode Materials. *Advanced Functional Materials* **2018**,*28* (30), 1800757.

References

1. Conway, B. E., Electrochemical supercapacitors: scientific fundamentals and technological applications. Springer Science & Business Media: **2013**.
2. Linden, D.; Reddy, T. B., Handbook of Batteries. 3rd. *McGraw-Hill* **2002**.
3. Zhu, Y.; Murali, S.; Stoller, M. D.; Ganesh, K.; Cai, W.; Ferreira, P. J.; Pirkle, A.; Wallace, R. M.; Cychosz, K. A.; Thommes, M., Carbon-based supercapacitors produced by activation of graphene. *Science* **2011**, *332* (6037),1537-1541.
4. Shukla, A.; Sampath, S.; Vijayamohanan, K., Electrochemical supercapacitors: Energy storage beyond batteries. *Curr. Sci.* **2000**, *79* (12),1656-1661.
5. Kate, R. S.; Khalate, S. A.; Deokate, R. J., Overview of nanostructured metal oxides and pure nickel oxide (NiO) electrodes for supercapacitors: a review. *J. Alloys Compd.* **2018**, *734*,89-111.
6. Saha, S.; Samanta, P.; Murmu, N. C.; Kuila, T., A review on the heterostructure nanomaterials for supercapacitor application. *J. Energy Storage* **2018**, *17*,181-202.
7. Yoo, J. J.; Balakrishnan, K.; Huang, J.; Meunier, V.; Sumpter, B. G.; Srivastava, A.; Conway, M.; Mohana Reddy, A. L.; Yu, J.; Vajtai, R., Ultrathin planar graphene supercapacitors. *Nano lett.* **2011**, *11* (4),1423-1427.
8. Xie, J.; Yang, P.; Wang, Y.; Qi, T.; Lei, Y.; Li, C. M., Puzzles and confusions in supercapacitor and battery: Theory and solutions. *J. Power Sources* **2018**, *401*, 213-223.
9. Huang, M.; Li, F.; Dong, F.; Zhang, Y. X.; Zhang, L. L., MnO₂-based nanostructures for high-performance supercapacitors. *J. Mater. Chem. A.* **2015**, *3* (43),21380-21423.
10. Conway, B.; Birss, V.; Wojtowicz, J., The role and utilization of pseudocapacitance for energy storage by supercapacitors. *J. Power Sources* **1997**, *66* (1-2),1-14.
11. Chen, G. Z., Supercapacitor and supercapattery as emerging electrochemical energy stores. *Int. Mater. Rev.* **2017**, *62* (4),173-202
12. Zhi, M.; Xiang, C.; Li, J.; Li, M.; Wu, N., Nanostructured carbon–metal oxide composite electrodes for supercapacitors: a review. *Nanoscale* **2013**, *5* (1),72-88.

13. Dubal, D. P.; Ayyad, O.; Ruiz, V.; Gomez-Romero, P., Hybrid energy storage: the merging of battery and supercapacitor chemistries. *Chem. Soc. Rev.* **2015**, *44* (7), 1777-1790.
14. Wang, G.; Zhang, L.; Zhang, J., A review of electrode materials for electrochemical supercapacitors. *Chem. Soc. Rev.* **2012**, *41* (2), 797-828.
15. Dang, Y.-Q.; Ren, S.-Z.; Liu, G.; Cai, J.; Zhang, Y.; Qiu, J., Electrochemical and capacitive properties of carbon dots/reduced graphene oxide supercapacitors. *Nanomater.* **2016**, *6* (11),212.
16. Klumpp, C.; Kostarelos, K.; Prato, M.; Bianco, A., Functionalized carbonnanotubes as emerging nanovectors for the delivery of. therapeutics.*Biochimica et biophysica acta. Biomembranes***2006**, *1758* (3),404-412
17. Pandey, P.; Dahiya, M., Carbon nanotubes: Types, methods of preparation and applications. *Carbon* **2016**, *1* (4).
18. Farzana, R.; Rajarao, R.; Bhat, B. R.; Sahajwalla, V., Performance of an activated carbon supercapacitor electrode synthesised from waste Compact Discs (CDs). *J. Ind. Eng. Chem.* **2018**; , *187*(1-3)
19. Allen,M.J.;Tung,V.C.;Kaner,R.B.,Honeycombcarbon:areviewofgraphene. *Chem. Rev.* **2009**, *110* (1), 132-145.
20. Ke, Q.; Wang, J., Graphene-based materials for supercapacitorelectrodes–A review. *J. Materiomics***2016**, *2* (1), 37-54.
21. Rowley-Neale, S. J.; Randviir, E. P.; Dena, A. S. A.; Banks, C. E., An overview of recent applications of reduced graphene oxide as a basis of electroanalytical sensing platforms. *Appl. Mater. Today* **2018**, *10*,218-226.
22. Yang, H.; Kannappan, S.; Pandian, A. S.; Jang, J.-H.; Lee, Y. S.; Lu, W., Graphene supercapacitor with both high power and energy density. *Nanotechnology* **2017**, *28* (44),445401.
23. Wang, H.; Hao, Q.; Yang, X.; Lu, L.; Wang, X., A nanostructured graphene/polyaniline hybrid material for supercapacitors. *Nanoscale* **2010**, *2* (10), 2164-2170.
24. Krishnamoorthy, K.; Pazhamalai, P.; Kim, S. J., Ruthenium sulfide nanoparticles as a new pseudocapacitive material for supercapacitor. *Electrochim. Acta* **2017**, *227*, 85-94.

25. Zhang, Y.; Feng, H.; Wu, X.; Wang, L.; Zhang, A.; Xia, T.; Dong, H.; Li, X.; Zhang, L., Progress of electrochemical capacitor electrode materials: A review. *Int. J. Hydrogen Energy* **2009**, *34* (11), 4889-4899.
26. Rudge, A.; Davey, J.; Raistrick, I.; Gottesfeld, S.; Ferraris, J. P., Conducting polymers as active materials in electrochemical capacitors. *J. Power Sources* **1994**, *47* (1-2), 89-107.
27. Li, H.; Wang, J.; Chu, Q.; Wang, Z.; Zhang, F.; Wang, S., Theoretical and experimental specific capacitance of polyaniline in sulfuric acid. *J. Power Sources* **2009**, *190* (2), 578-586; (b) Eftekhari, A.; Li, L.; Yang, Y., Polyaniline supercapacitors. *J. Power Sources* **2017**, *347*,86-107.
28. Adhikari, A. D.; Oraon, R.; Tiwari, S. K.; Saren, P.; Lee, J. H.; Kim, N. H.; Nayak, G. C., CdS-CoFe₂O₄@ Reduced Graphene Oxide Nanohybrid: An Excellent Electrode Material for Supercapacitor Applications. *Ind. Eng. Chem. Res.* **2018**, *57* (5), 1350-1360.
29. Ohno, H.; Fukumoto, K., Progress in ionic liquids for electrochemical reaction matrices. *Electrochemistry* **2008**, *76* (1), 16-23; (b) Galiński, M.; Lewandowski, A.; Stępnia, I., Ionic liquids as electrolytes. *Electrochim. Acta* **2006**, *51* (26),5567-5580.
30. Bard, A.; Faulkner, L., *Electrochemical methods: fundamentals and applications*. 2001, Hoboken. NJ: John Wiley & Sons, Inc.
31. Chen, G. Z., Understanding supercapacitors based on nano-hybrid materials with interfacial conjugation. *Prog. Nat. Sci.: Mater. Int.* **2013**, *23* (3),245-255.
32. Moussa, M.; El-Kady, M. F.; Zhao, Z.; Majewski, P.; Ma, J., Recent progress and performance evaluation for polyaniline/graphene nanocomposites as supercapacitor electrodes. *Nanotechnology* **2016**, *27* (44),442001.
33. Xu, P.; Liu, J.; Yan, P.; Miao, C.; Ye, K.; Cheng, K.; Yin, J.; Cao, D.; Li, K.; Wang, G., Preparation of porous cadmium sulphide on nickel foam: a novel electrode material with excellent supercapacitor performance. *J. Mater. Chem. A.* **2016**, *4* (13), 4920-4928.
34. Nair, N.; Sankapal, B. R., Nested CdS@ HgS core-shell nanowires as supercapacitive Faradaic electrode through simple solution chemistry. *Nano-Struc. Nano-Objects* **2017**, *10*,159-166.
35. Patil, D. S.; Pawar, S. A.; Shin, J. C., Core-shell structure of Co₃O₄@ CdS for high performance electrochemical supercapacitor. *Chem. Eng. J.* **2018**, *335*,693-702.

36. Chen, L.; Zuo, Y.; Zhang, Y.; Gao, Y., Cadmium sulfide anchored in three-dimensional graphite cage for high performance supercapacitors. *Appl. Phys. Lett.* **2018**, *112* (22),223901.
37. Patil, D. S.; Pawar, S. A.; Shin, J. C., Alteration of Ag nanowires to Ag/Ag₂S nanowires@ CdS core-shell architectures for electrochemical supercapacitors. *J. Alloys Compd.* **2018**, *768*,1076-1082.
38. Arbizzani, C.; Mastragostino, M.; Meneghello, L., Polymer-based redox supercapacitors: A comparative study. *Electrochim. Acta* **1996**, *41* (1),21-26.
39. Ryu, K. S.; Kim, K. M.; Park, N.-G.; Park, Y. J.; Chang, S. H., Symmetric redox supercapacitor with conducting polyaniline electrodes. *J. Power Sources* **2002**, *103* (2),305-309.
40. Chen, W.-C.; Wen, T.-C.; Teng, H., Polyaniline-deposited porous carbon electrode for supercapacitor. *Electrochim. Acta* **2003**, *48* (6),641-649.
41. Gupta, V.; Miura, N., High performance electrochemical supercapacitor from electrochemically synthesized nanostructured polyaniline. *Mater. Lett.* **2006**, *60* (12), 1466-1469.
42. Dhawale, D.; Vinu, A.; Lokhande, C., Stable nanostructured polyaniline electrode for supercapacitor application. *Electrochim. Acta* **2011**, *56* (25),9482-9487.
43. Khadry, N. H.; Abdesalam, M. E.; Enany, G. E., Mesoporous polyaniline films for high performance supercapacitors. *J. Electrochem. Soc.* **2014**, *161* (9),G63-G68.
44. Feng, X. M.; Li, R. M.; Ma, Y. W.; Chen, R. F.; Shi, N. E.; Fan, Q. L.; Huang, W., One-step electrochemical synthesis of graphene/polyaniline composite film and its applications. *Adv. Funct. Mater.* **2011**, *21* (15), 2989-2996.
45. Ma, B.; Zhou, X.; Bao, H.; Li, X.; Wang, G., Hierarchical composites of sulfonated graphene-supported vertically aligned polyaniline nanorods for high-performance supercapacitors. *J. Power Sources* **2012**, *215*,36-42.
46. Yu, L.; Gan, M.; Ma, L.; Huang, H.; Hu, H.; Li, Y.; Tu, Y.; Ge, C.; Yang, F.; Yan, J., Facile synthesis of MnO₂/polyaniline nanorod arrays based on graphene and its electrochemical performance. *Synth. Met.* **2014**, *198*,167-174.
47. Das, A. K.; Karan, S. K.; Khatua, B., High energy density ternary composite electrode material based on polyaniline (PANI), molybdenum trioxide (MoO₃) and graphene nanoplatelets (GNP) prepared by sono-chemical method and their synergistic contributions in superior supercapacitive performance. *Electrochim. Acta* **2015**, *180*, 1-15.

48. Li, X.; Zhang, C.; Xin, S.; Yang, Z.; Li, Y.; Zhang, D.; Yao, P., Facile synthesis of MoS₂/reduced graphene oxide@ polyaniline for high-performance supercapacitors. *ACS Appl Mater. Interfaces* **2016**, *8* (33),21373-21380.
49. Purty, B.; Choudhary, R.; Biswas, A.; Udayabhanu, G., Potentially enlarged supercapacitive values for CdS-PPY decorated rGO nanocomposites as electrode materials. *Mater. Chem. Phy.***2018**.
50. Cazes, J., *Analytical instrumentation handbook*. CRC Press:2004.
51. Bertin, E. P., *Principles and practice of X-ray spectrometric analysis*. Springer Science & Business Media:2012.
52. Skoog, D. A.; Holler, F. J.; Crouch, S. R., *Principles of instrumental analysis*. Cengage learning:2017.
53. Xiang, Z.; Nan, J.; Deng, J.; Shi, Y.; Zhao, Y.; Zhang, B.; Xiang, X., Uniform CdS- decorated carbon microsheets with enhanced photocatalytic hydrogen evolution under visible-light irradiation. *J. Alloys Compd.* **2019**, *770*,886-895.
54. Al-Fahdi, T.; Al Marzouqi, F.; Kuvarega, A. T.; Mamba, B. B.; Al Kindy, S. M.; Kim, Y.; Selvaraj, R., Visible light active CdS@ TiO₂ core-shell nanostructures for the photodegradation of chlorophenols. *J. Photochem. Photobiol., A***2019**.
55. Talbi, L.; Berouaken, M.; Khaldi, K.; Keffous, A.; Gabouze, N.; Trari, M.; Menari, H.; Belkacem, Y., Elaboration and characterization of electrochemically prepared H⁺- doped polyaniline/Au/a-SiC: H-based chemical sensor. *J. Solid State Electrochem.* **2018**, *22* (4),1123-1130.
56. Habibi, M. H.; Rahmati, M. H., Fabrication and characterization of ZnO@ CdS core– shell nanostructure using acetate precursors: XRD, FESEM, DRS, FTIR studies and effects of cadmium ion concentration on band gap. *Spectrochim. Acta, Part A* **2014**, *133*, 13-18; (b) Wang, H.; Fang, P.; Chen, Z.; Wang, S., Synthesis and characterization of CdS/PVA nanocomposite films. *Appl. Surf. Sci.* **2007**, *253* (20), 8495-8499.
57. Mishra, N.; Shinde, S.; Vishwakarma, R.; Kadam, S.; Sharon, M.; Sharon, M. In MWCNTs synthesized from waste polypropylene plastics

- and its application in super- capacitors, *AIP Conf. Proc.***2013**;228-236.
58. Li, H.; Lang, J.; Lei, S.; Chen, J.; Wang, K.; Liu, L.; Zhang, T.; Liu, W.; Yan, X., A High Performance Sodium -Ion Hybrid Capacitor Constructed by Metal–Organic Framework–Derived Anode and Cathode Materials. *Adv. Funct. Mater.***2018**, 28 (30),1800757.